ZHEJIANG UNIVERSITY

Avec le soutien de la Wallonie

fnrs LA LIBERTÉ DE CHERCHER

LIÈGE université Urban & Environmental Engineering

Second gradient model for the modelling of strain localization process: from the laboratory experiment to the numerical modelling of nuclear waste disposal

Frédéric COLLIN, Benoit PARDOEN, Gilles CORMAN, Hangbiao SONG

21-05-2025

This work is co-funded by the FNRS – Projet bilateral de Mobilité PINT-BILAT-M R.M008.23

Context

Failure in soils and rocks is almost always associated with fractures and/or shear bands developing in the geomaterial.

Shear banding occurs frequently (at many scales) and is the source of many soil and rock engineering problems:

natural or human-made slopes or excavations, unstable rock masses, embankments or dams, tunnels and mine galleries, boreholes driven for oil production, repositories for nuclear waste disposal

Context

In situ observations of shear banding and/or faulting are made frequently at many scales

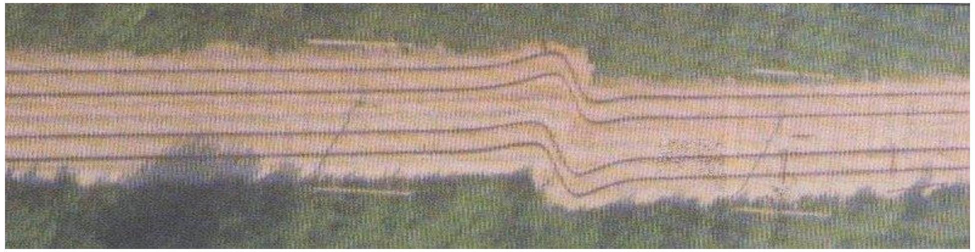

Large scale: railway tracks after an earthquake in Turkey

Context

In situ observations of shear banding and/or faulting are made frequently at many scales

Human-made slope along E42 exit road

Context

In situ observations of shear banding and/or faulting are made frequently at many scales

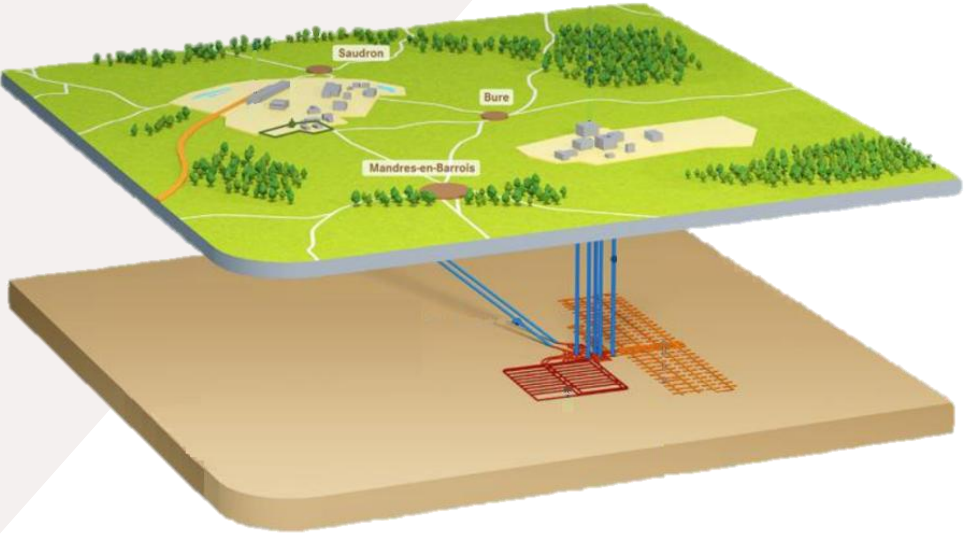

Nuclear waste storage

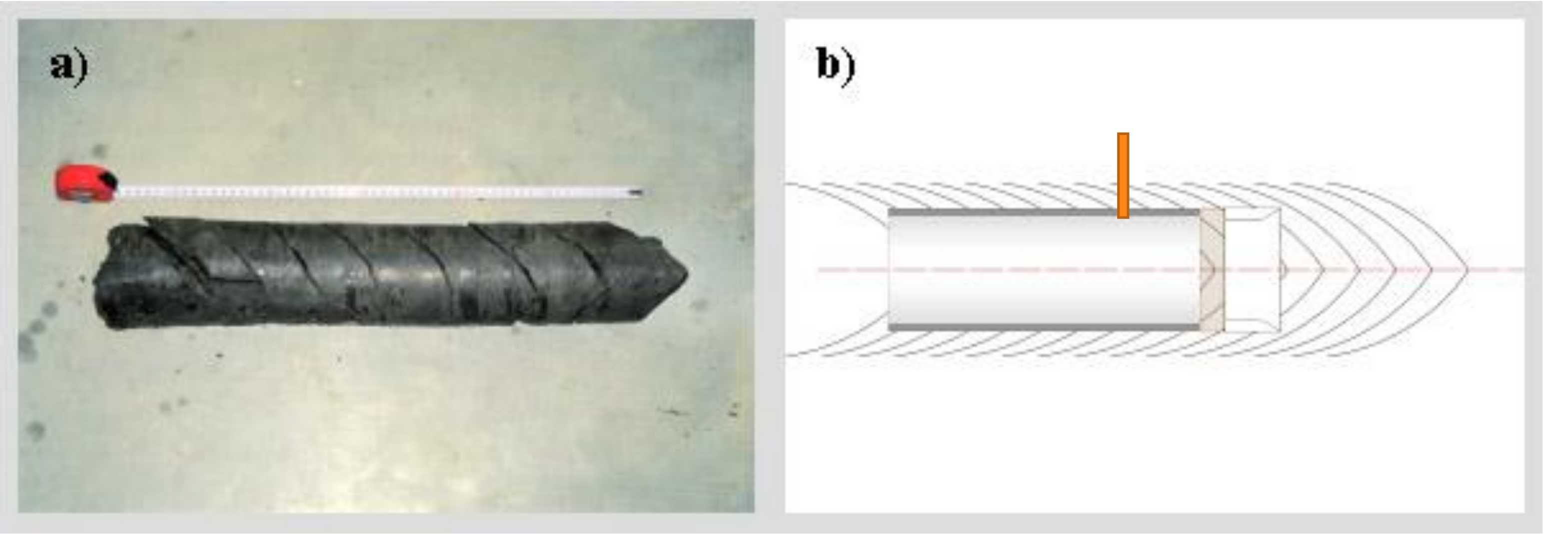

Fractures observed during the construction of the connecting gallery at the URL in Mol. Vertical cross section through the gallery showing the fracturation pattern around it, as deduced from the observations (from Alheid et al. 2005)

Context

In situ observations of shear banding and/or faulting are made frequently at many scales

Localized rupture in sandstone samples under different confining pressures (Bésuelle et al., 2000)

Experimental characterisation of the localisation phenomenon inside a Vosges sandstone in a triaxial cell
P. BESUELLE, J. DESRUES, S. RAYNAUD, International Journal of Rock Mechanics & Mining Sciences 37 (2000) p. 1223-1237

Context

In situ observations of shear banding and/or faulting are made frequently at many scales

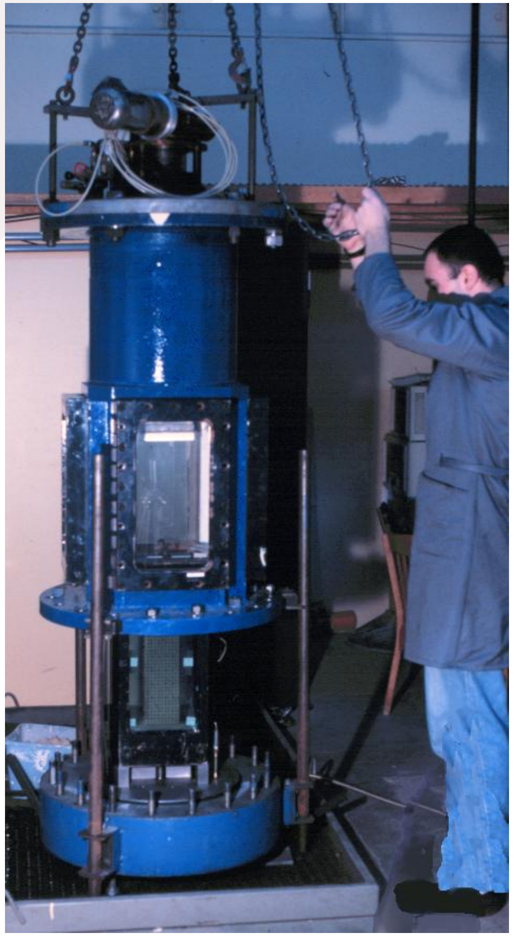

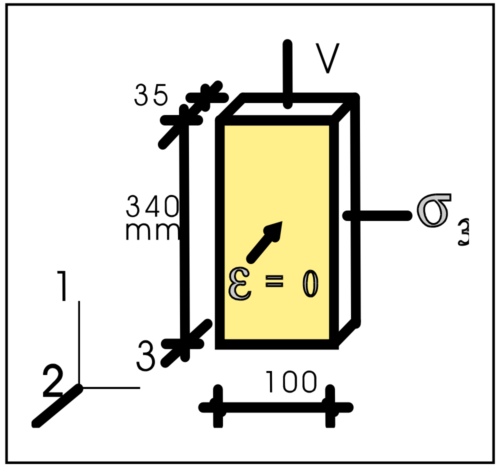

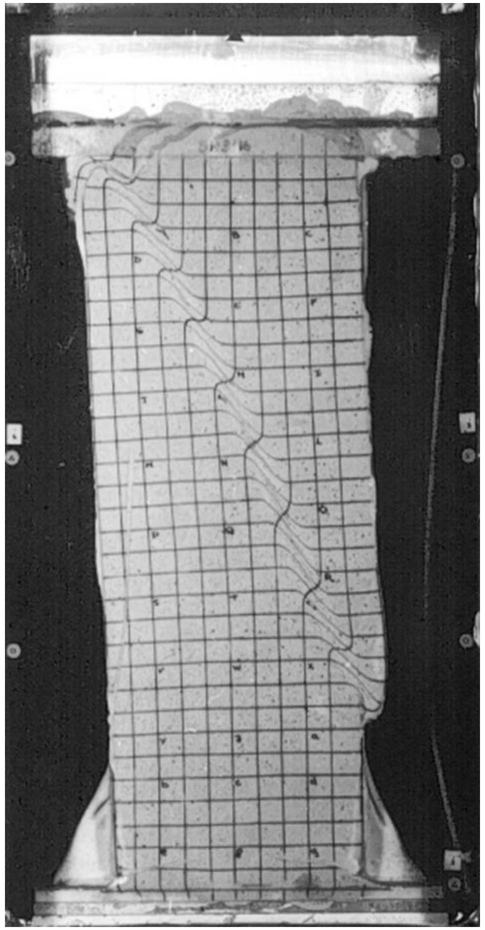

Experimental set-up of a biaxial test

Context

Failure in soils and rocks is almost always associated with fractures and/or shear bands developing in the geomaterial.

Shear banding occurs frequently (at many scales) and is the source of many soil and rock engineering problems:

natural or human-made slopes or excavations, unstable rock masses, embankments or dams, tunnels and mine galleries, boreholes driven for oil production, repositories for nuclear waste disposal

In geomaterials, the understanding of failure processes is more complex by the fact that soils and rocks are multiphase porous materials where different multiphysical processes take place.

Context

“ Are we able to model the rupture process in geomaterials? ”

- Theoretical approach:
  - Focus on the rupture in localized mode ;
  - Rice criterion to predict the onset of localization.
- Numerical approach:
  - Development of a second gradient model for a robust prediction of the post peak regime;
  - Extension to HM second gradient model
- Application:
  - Underground nuclear waste disposal.

Table of Contents

LIÈGE université
Urban & Environmental Engineering

Context

Rupture accross the scale

Theoretical Approach

Localized mode of deformation

Numerical Approach

Second gradient model

Application

Underground nuclear waste disposal

Experimental Evidence

Localized mode of failure

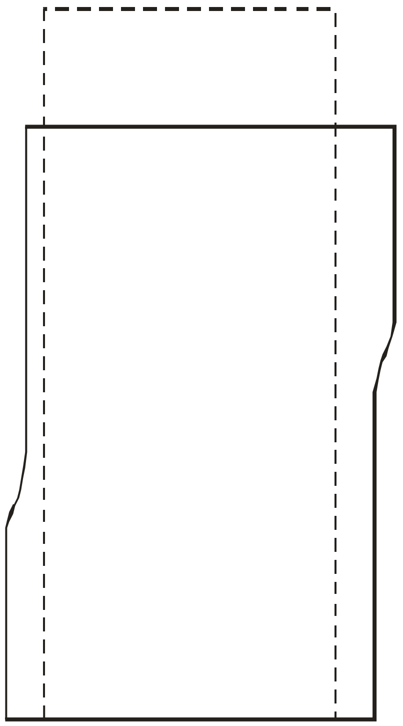

Initial state *Homogeneous strain field* *Localized strain field*

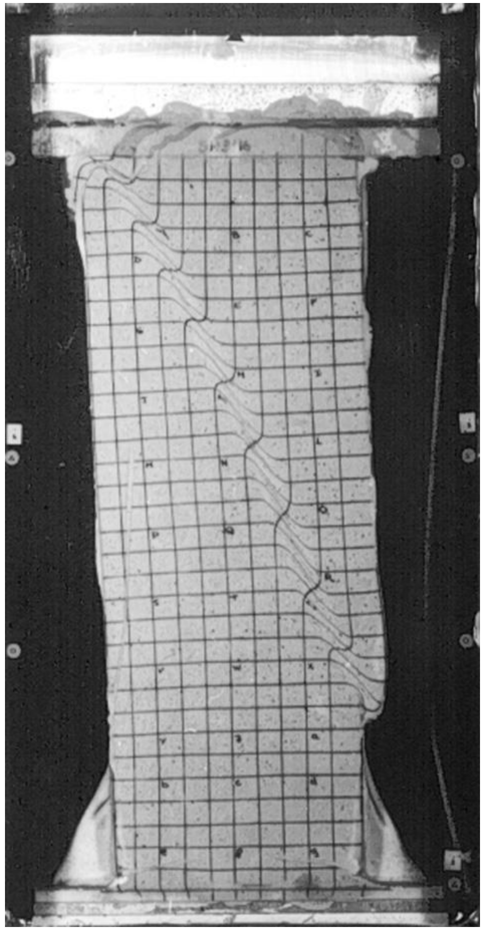

Theoretical approach

Theoretical background

Following the previous works by (Hadamard, 1903), (Hill, 1958) and (Mandel, 1966), Rice and co-workers (Rice, 1976, Rudnicki et al., 1975) have proposed the so-called **Rice criterion**.

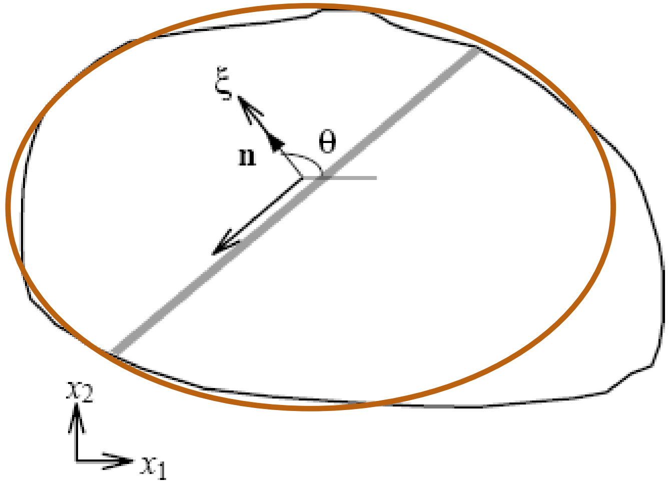

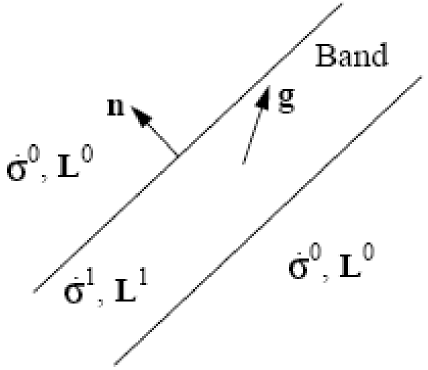

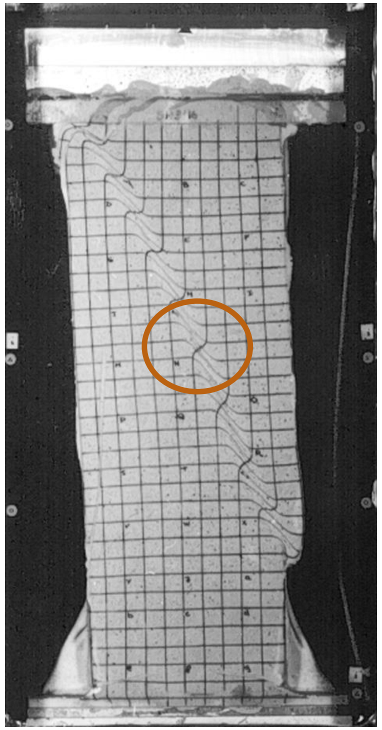

Theoretical approach

Rice criterion

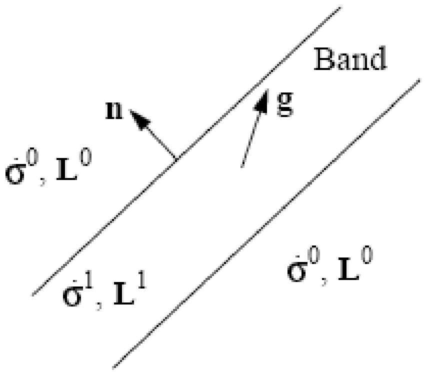

$$L_{ij} = \frac{1}{2}\left(\frac{\partial \dot{u}_i}{\partial x_j} + \frac{\partial \dot{u}_j}{\partial x_i}\right)$$

Static condition: $n\left(\dot{\sigma}^1 - \dot{\sigma}^0\right) = 0$

Kinematic condition: $L^1 = L^0 + \Delta L$

$$L^1 = L^0 + g \otimes n$$

Constitutive law: $\dot{\sigma} = C : L$

Theoretical approach

Rice criterion

Constitutive law in principal axis:

$$\begin{Bmatrix} \dot{\sigma}_{11} \\ \dot{\sigma}_{22} \\ \dot{\sigma}_{12} \end{Bmatrix} = \begin{bmatrix} C_{11} & C_{12} & 0 \\ C_{21} & C_{22} & 0 \\ 0 & 0 & 2G_{12} \end{bmatrix} \begin{Bmatrix} L_{11} \\ L_{22} \\ L_{12} \end{Bmatrix}$$

Static condition:

$$\left(\dot{\sigma}_{ij}^{1} - \dot{\sigma}_{ij}^{0}\right) n_j = 0$$

$$\begin{cases} \left(\dot{\sigma}_{11}^{1} - \dot{\sigma}_{11}^{0}\right) n_1 + \left(\dot{\sigma}_{12}^{1} - \dot{\sigma}_{12}^{0}\right) n_2 = 0 \\ \left(\dot{\sigma}_{21}^{1} - \dot{\sigma}_{21}^{0}\right) n_1 + \left(\dot{\sigma}_{22}^{1} - \dot{\sigma}_{22}^{0}\right) n_2 = 0 \end{cases}$$

Kinematic condition:

$$L_{ij}^{1} = L_{ij}^{0} + g_i n_j$$

Theoretical approach

Rice criterion

Combining the three previous relationship yields:

If $C^1 = C^0 = C$:

$$\begin{cases} \left(C_{11}g_1n_1 + C_{12}g_2n_2\right)n_1 + G_{12}\left(g_1n_2 + g_2n_1\right)n_2 = 0 \\ G_{12}\left(g_1n_2 + g_2n_1\right)n_1 + \left(C_{21}g_1n_1 + C_{22}g_2n_2\right)n_2 = 0 \end{cases}$$

$$\begin{cases} \left(C_{11}n_1^{\,2} + G_{12}n_2^{\,2}\right)g_1 + \left(C_{12}n_1n_2 + G_{12}n_2n_1\right)g_2 = 0 \\ \left(C_{21}n_1n_2 + G_{12}n_2n_1\right)g_1 + \left(C_{22}n_2^{\,2} + G_{12}n_1^{\,2}\right)g_2 = 0 \end{cases}$$

When it is assumed that $C^1 = C^0 = C$, no trivial solution if and only if: $\det(nCn) \leq 0$

$$\left(C_{11}G_{12}\right)n_1^{\,4} + \left(C_{22}G_{12}\right)n_2^{\,4} + \left(C_{11}C_{22} - 2C_{12}G_{12} - C_{12}^2\right)n_1^{\,2}n_2^{\,2} = 0$$

Theoretical approach

Rice criterion

Defining $z = \frac{n_2}{n_1}$*, the previous equation can be rewritten as:*

$$n_1^4 \left(a_1 z^4 + a_3 z^2 + a_5 \right) = 0$$

For a constitutive law written in cartesian axis:

$$n_1^4 \left(a_1 z^4 + a_2 z^3 + a_3 z^2 + a_4 z + a_5 \right) = 0$$

Theoretical approach

Extension to multiphysical context, mainly in hydro mechanical coupling:

Loret and co-workers (Loret et al., 1991) showed that for hydromechanical problems the condition of localization depends only on the **drained properties** of the medium

In coupled problems much more **complex localization pattern** can be obtained, at least theoretically (Vardoulakis, 1996)

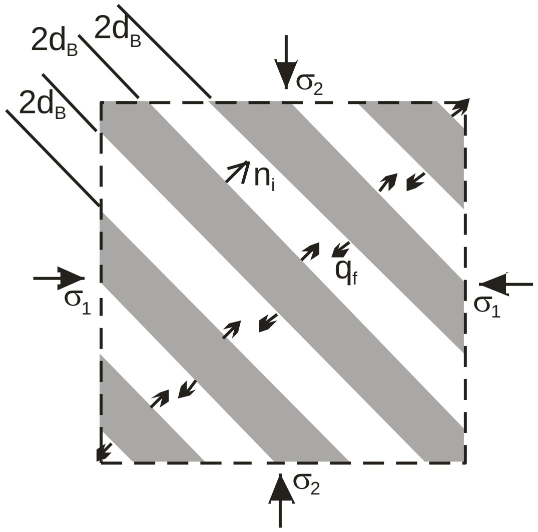

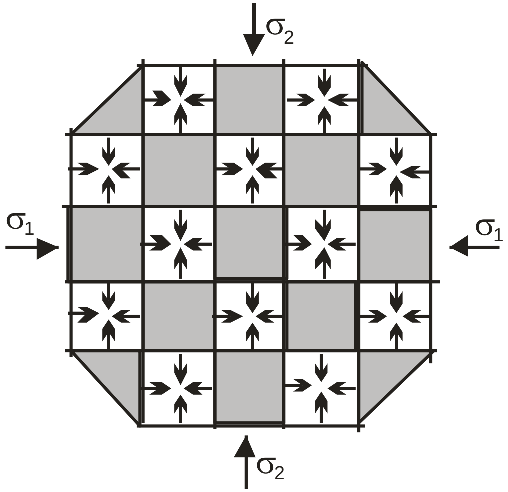

Theoretical approach

Which information can provide this theoretical criterion ?

For element test, the Rice criterion allow us to check if and when the constitutive model is able to predict the localization direction observed at the laboratory.

For boundary value problems, they provide the stress state when bifurcation may arise and the direction of potential bifurcation (fracturation). Be aware that the Rice criterion is a local one !

Theoretical approach

Example n°1: Biaxial test (homogeneous case)

Mechanical behaviour

Linear elasticity : E_0 *et* ν_0

Drucker Prager criterion : $$F \equiv \sqrt{\frac{3}{2}} II_{\hat{\sigma}} + m\left(I_\sigma - \frac{3c}{\tan\phi} \right) = 0$$

$$m = \frac{2\sin\phi}{3-\sin\phi} \qquad c = c_0\, f(\gamma^p)$$

Associated softening plasticity (decrease of cohesion) :

$$f(\gamma^p) = \left(1-(1-\alpha)\frac{\gamma^p}{\gamma^p_R} \right)^2 si\ 0 < \gamma^p < \gamma^p_R$$

$$= \alpha^2\ si\ \gamma^p \geq \gamma^p_R$$

Theoretical approach

Example n°1: Biaxial test (homogeneous case)

Softening behaviour : localization effects are very important

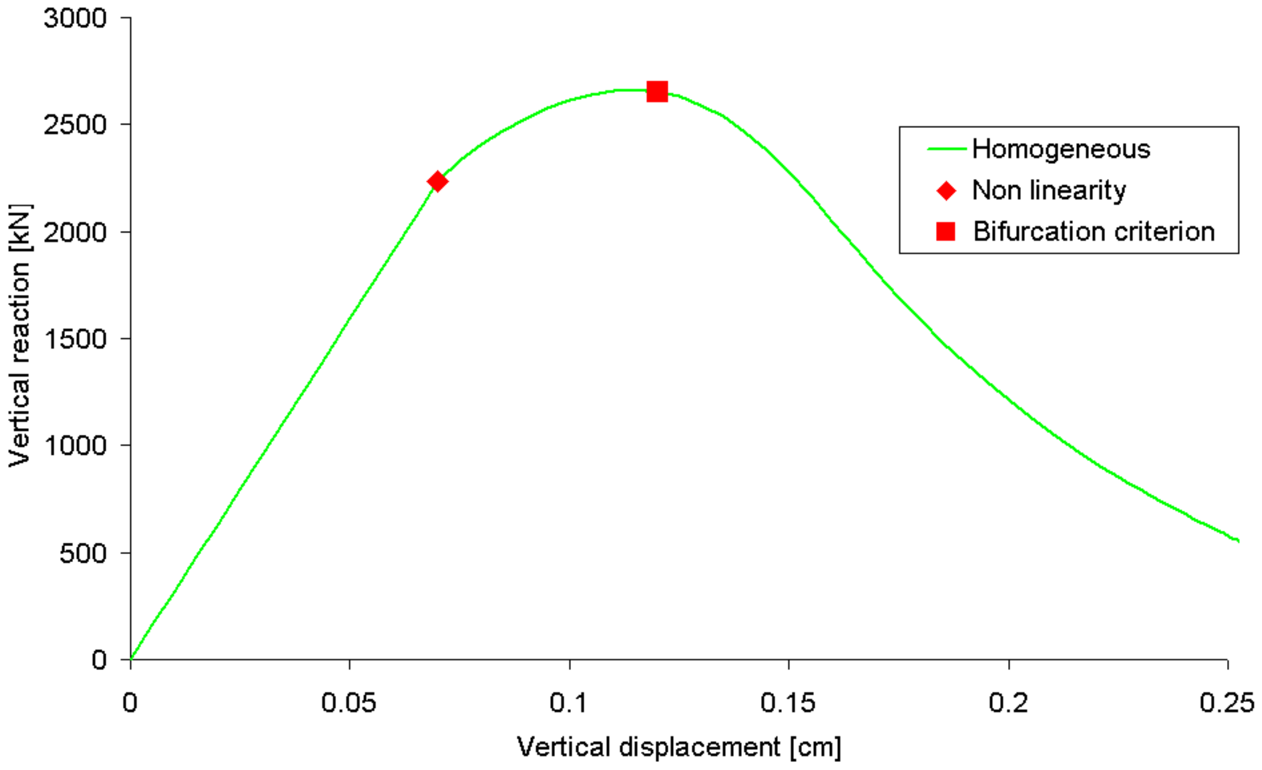

Theoretical approach

Example n°1: Biaxial test (homogeneous case)

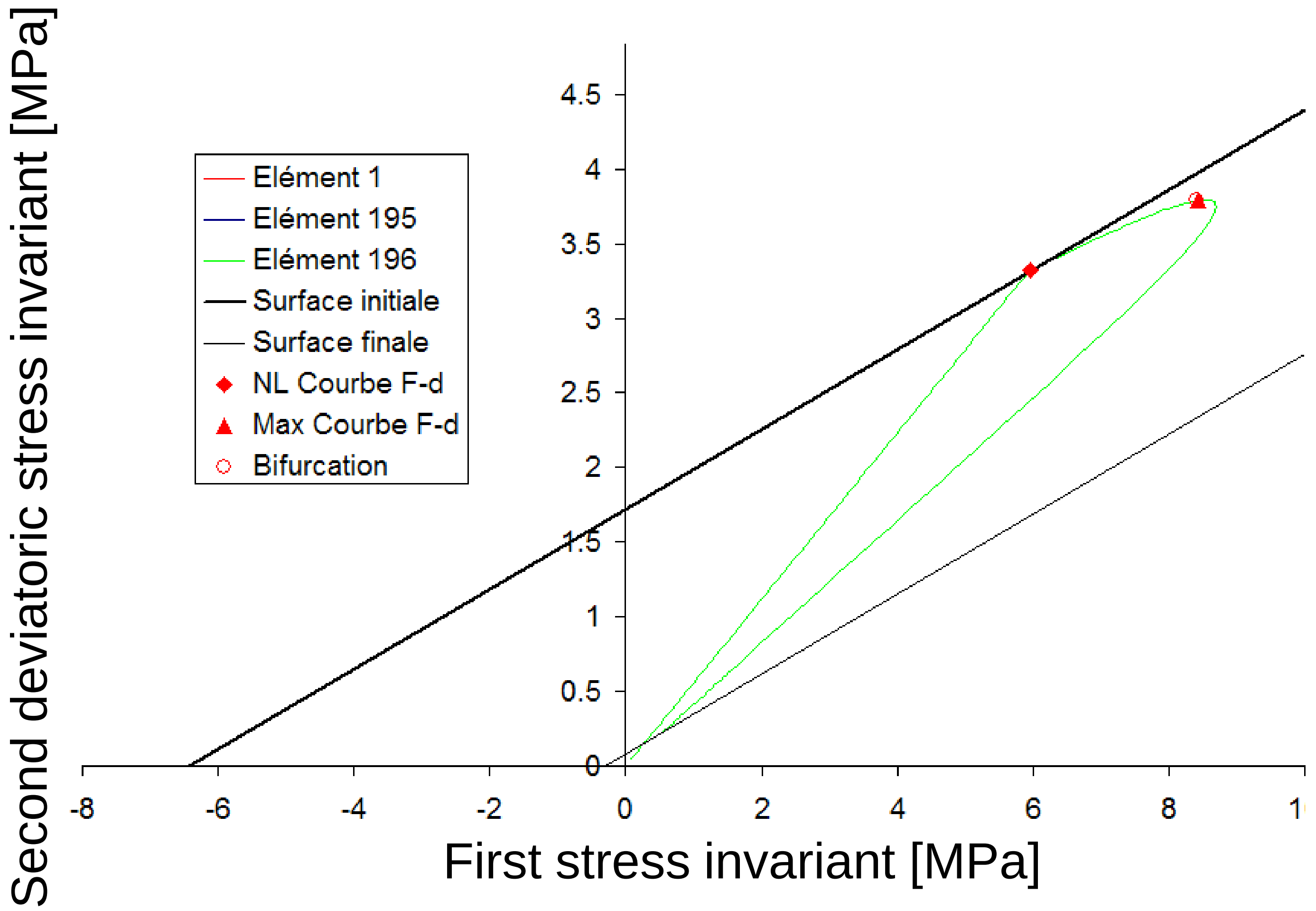

Theoretical approach

Example n°1: Biaxial test (homogeneous case)

$$\det\left(\underline{\Lambda}(\vec{n})\right) = n_1^4\left(a_1 z^4 + a_2 z^3 + a_3 z^2 + a_4 z + a_5\right) \leq 0$$

Acoustic tensor determinent

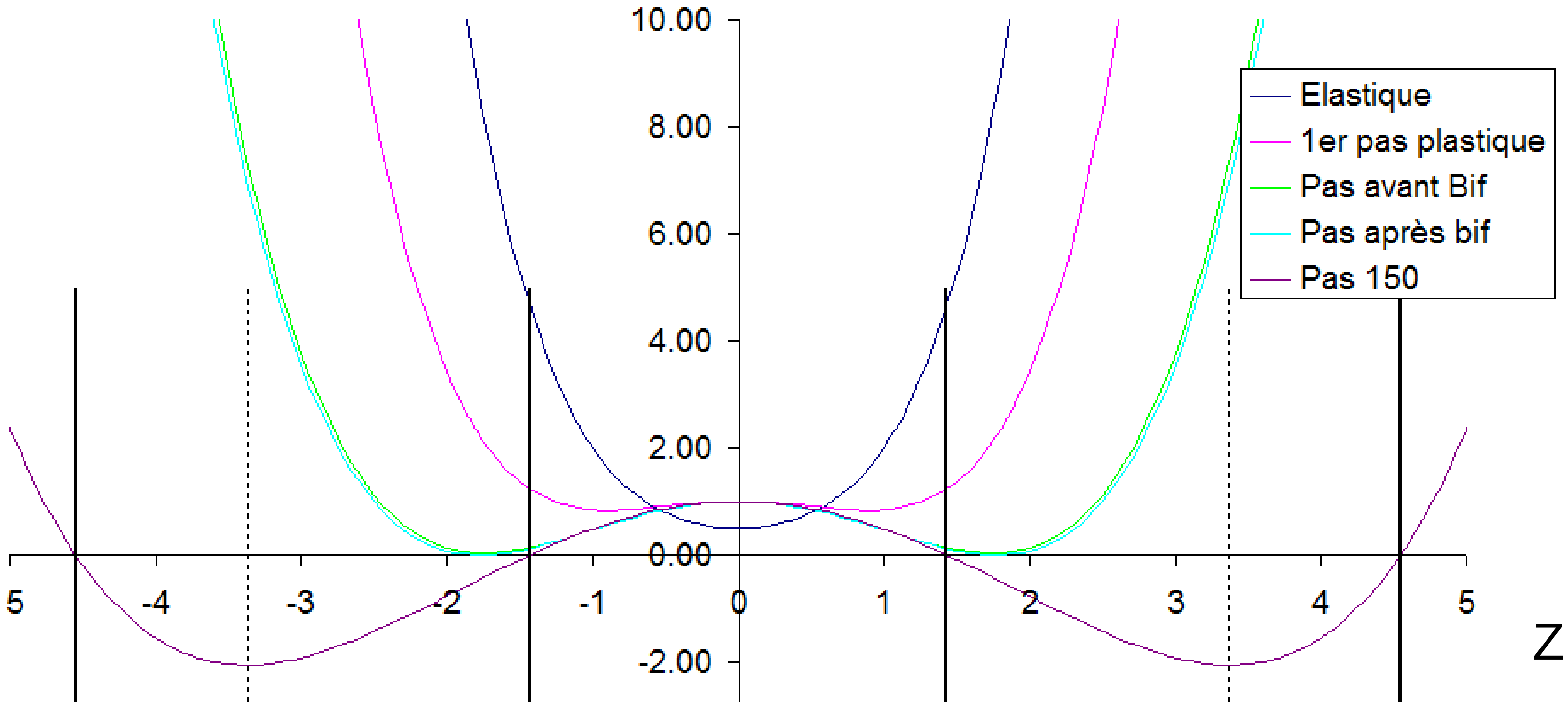

Theoretical approach

Example n°1: Biaxial test (homogeneous case)

Plastic point

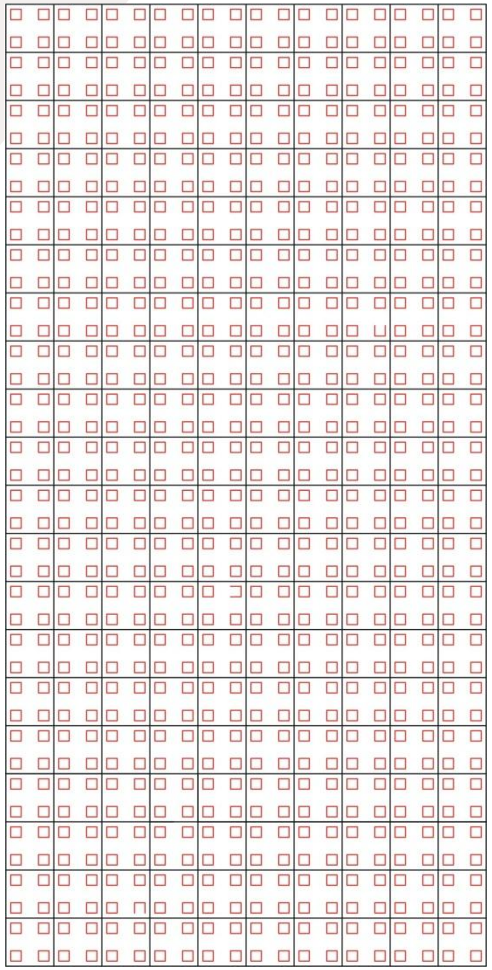

Bifurcation dir.

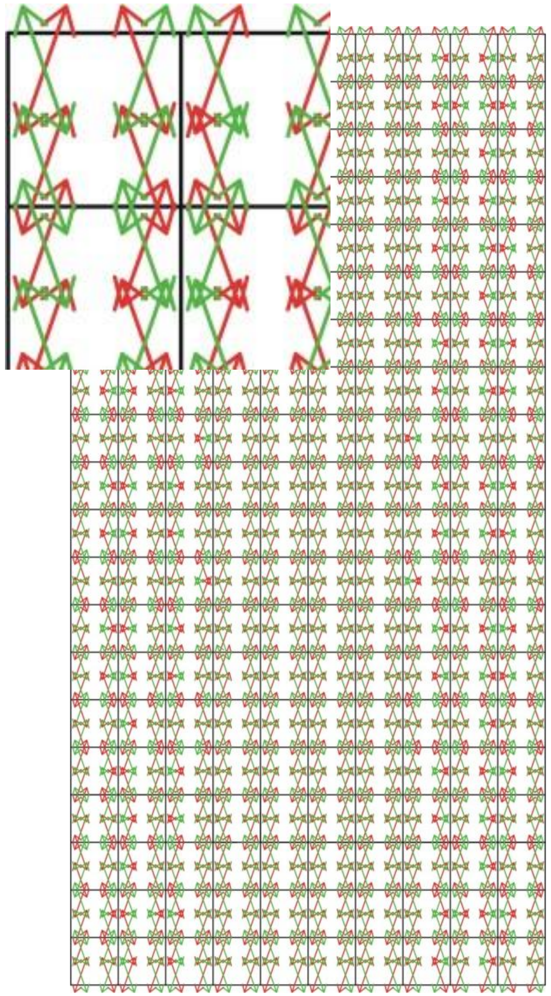

Bifurcation cones

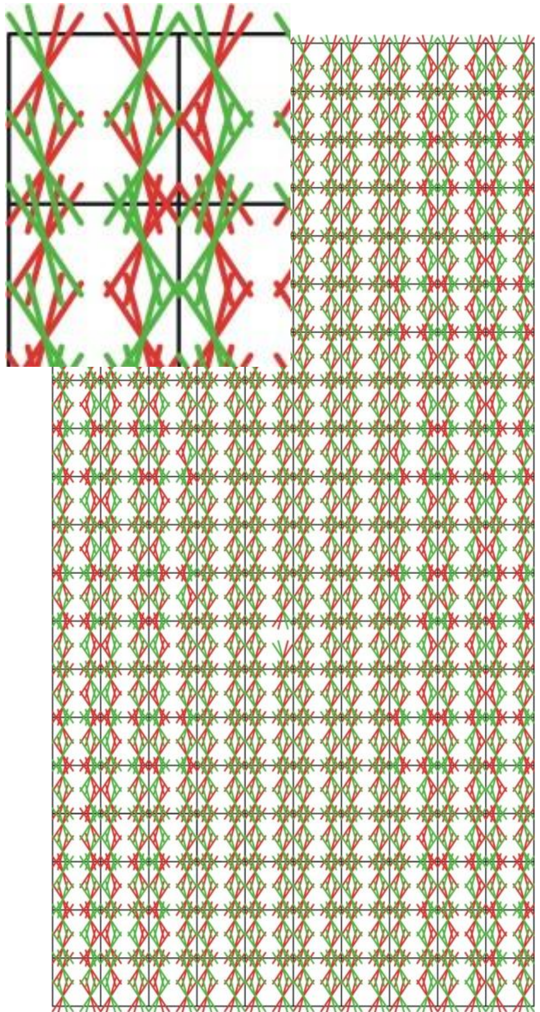

Theoretical approach

The Rice criterion provides us the information on when and how localization may appear. Do we have any problem to model such phenomenon with classical finite element method ?

Let's consider the modelling of a biaxial test with a defect triggering the localization, first without any hydromechanical effect.

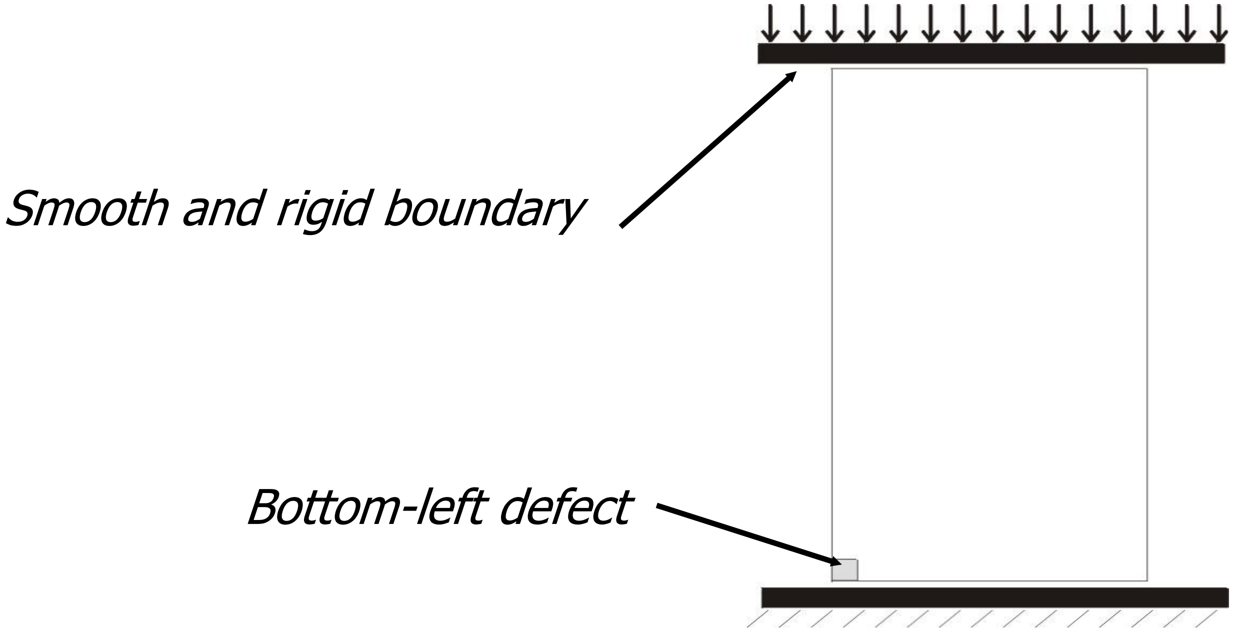

Theoretical approach

Example n°1: Biaxial test (localized case)

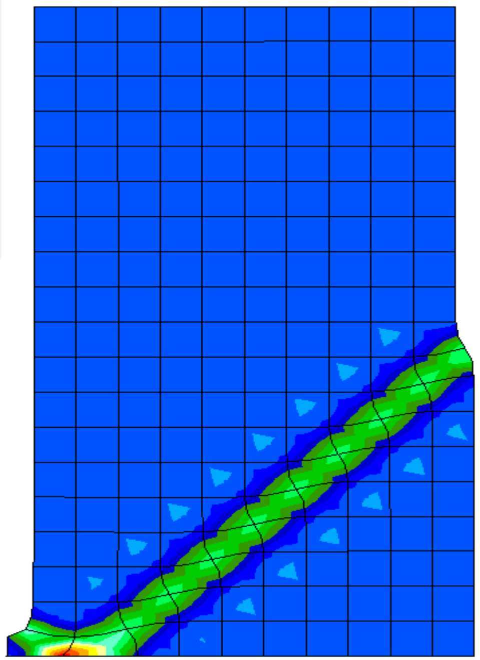

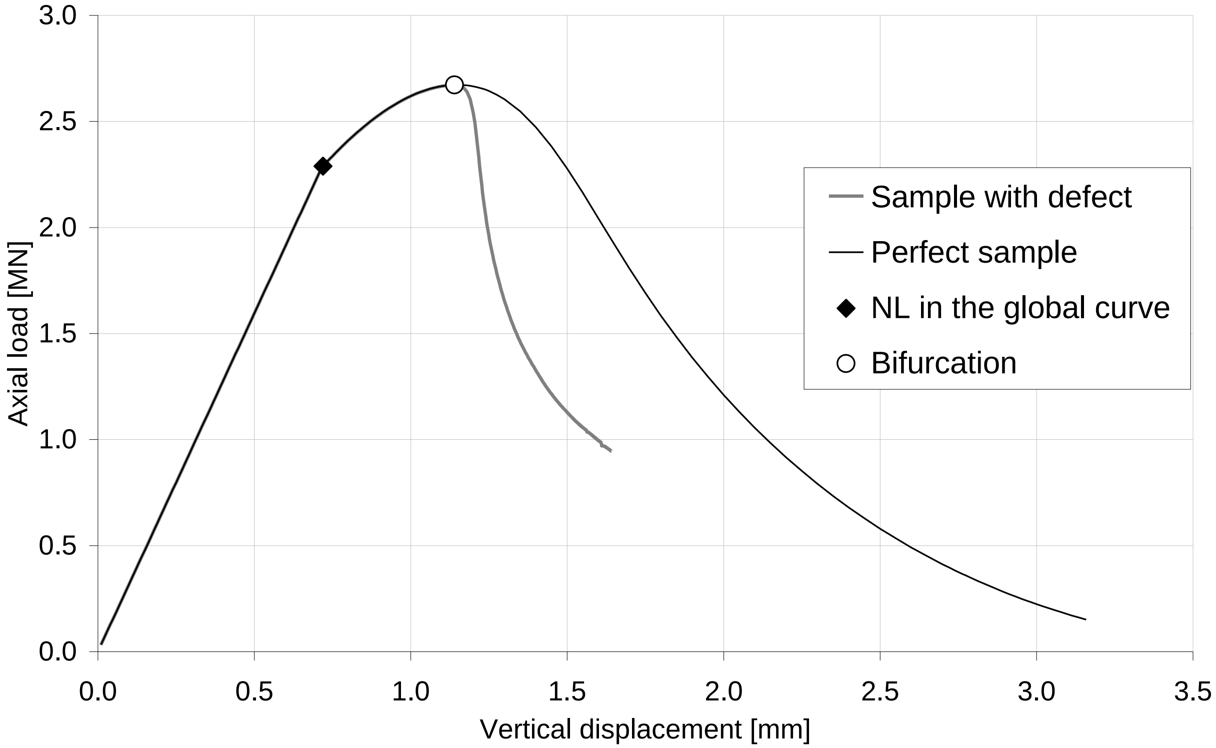

Theoretical approach

Example n°1: Biaxial test (localized case)

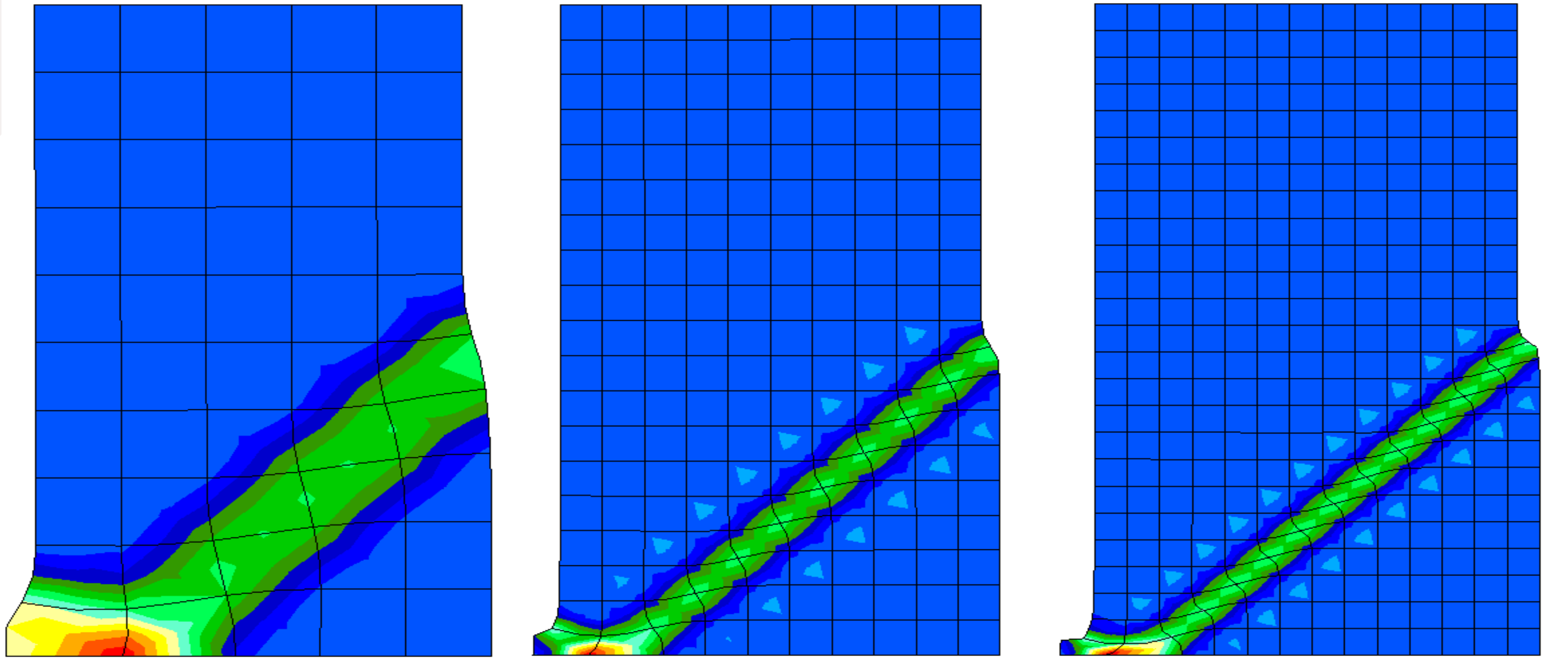

50 elements 200 elements 300 elements

The post peak behaviour depends on the mesh size !

Theoretical approach

Example n°2

Cylindrical cavity without lining structure

Anisotropic initial state of stress

Geometrical dimensions : *Internal radius 3 m*

Mesh length 60 m

Choice :

Symmetry of the problem is assumed

894 elements – 2647 nodes – 7941 dof

Theoretical approach

Example n°2

Coupled modelling – Comparison Coarse mesh / Refined mesh

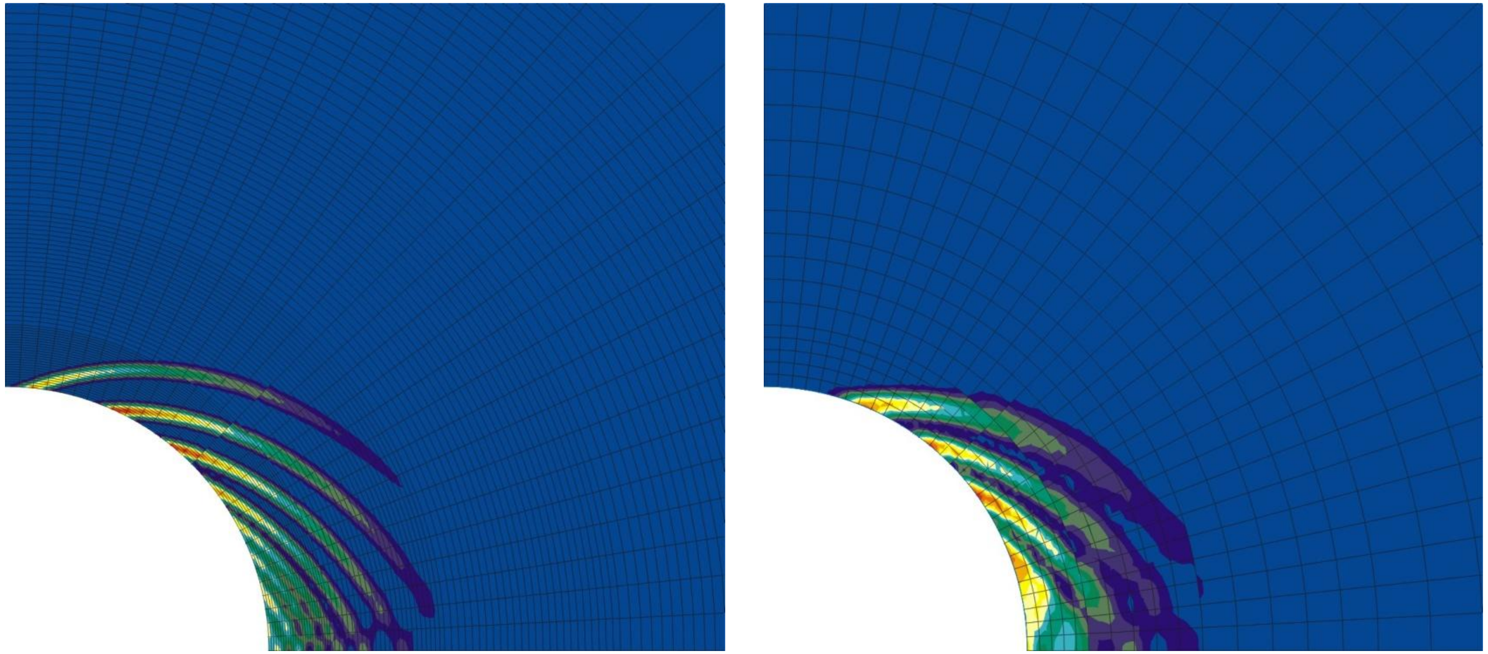

Deviatoric strains

Theoretical approach

LIÈGE université
Urban & Environmental Engineering

Conclusion

- Localization study : Acoustic tensor determinent
- Mesh dependency of the results for classical FE
- Non-uniqueness of the results in both cases

The numerical modelling of strain localization with classical FE is not adequate.

We need another numerical model to fix this mesh dependency problem !

Table of Contents

Numerical Approach

- Classical FE formulation: mesh dependency

- Different regularization methods

Gradient plasticity

Non-local approach

Enrichment of the law

Microstructure continuum

Cosserat model

Second gradient model

Enrichment of the kinematics

Mainly for monophasic materials !

Numerical Approach

In second gradient model, the continuum is enriched with microstructure effects. The kinematics include therefore the classical one but also microkinematics (See Germain 1973, Toupin 1962, Mindlin 1964).

Let us define first the classical kinematics:

- u_i is the (macro) displacement field
- F_{ij} is the macro displacement gradient which means:

$$F_{ij} = \frac{\partial u_i}{\partial x_j}$$

- D_{ij} is the macro strain:

$$D_{ij} = \frac{1}{2}(F_{ij} + F_{ji})$$

- R_{ij} is the macro rotation:

$$R_{ij} = \frac{1}{2}(F_{ij} - F_{ji})$$

Numerical Approach

Enrichment of the kinematics :

The continuum is enriched with microstructure effects: Macro-kinematics + micro-kinematics

Macro Ω:

$$F_{ij} = \frac{\partial u_i}{\partial x_j} = D_{ij} + R_{ij}$$

Micro Ω^m:

$$f_{ij} = \frac{\partial {u_i}^m}{\partial x_j} = {d_{ij}}^m + {r_{ij}}^m$$

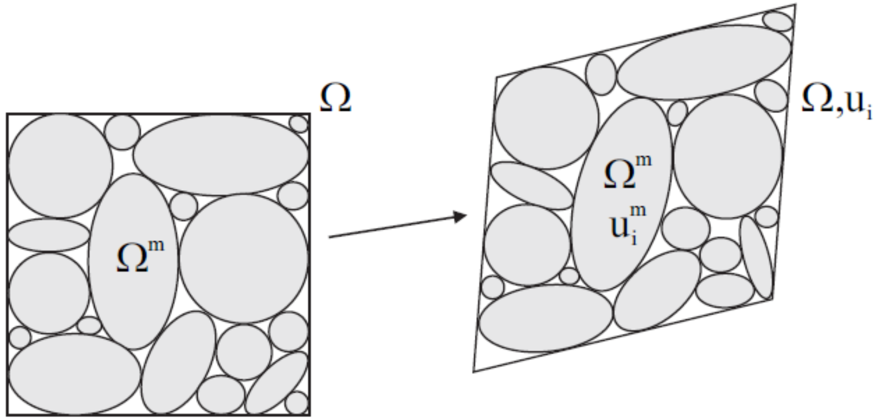

Numerical Approach

In second gradient model, the continuum is enriched with microstructure effects. The kinematics include therefore the classical one but also microkinematics (See Germain 1973, Toupin 1962, Mindlin 1964).

Let us define the micro-kinematics:

- f_{ij} is the microkinematic gradient.
- d_{ij} is the microstrain:

$$d_{ij} = \frac{1}{2}(f_{ij} + f_{ji})$$

- r_{ij} is the microrotation:

$$r_{ij} = \frac{1}{2}(f_{ij} - f_{ji})$$

- h_{ijk} is the (micro) second gradient:

$$h_{ijk} = \frac{\partial f_{ij}}{\partial x_k}$$

Numerical Approach

Second gradient model formulation: weak form

- The internal virtual work (Germain, 1973)

$$W^{*\mathrm{i}} = \int_{\Omega} w^{*}\,\mathrm{d}v = \int_{\Omega} \left(\sigma_{ij} D^{*}_{ij} + \tau_{ij}\left(f^{*}_{ij} - F^{*}_{ij}\right) + \chi_{ijk} h^{*}_{ijk}\right) \mathrm{d}v$$

- The external virtual work (simplified)

$$W^{*\mathrm{e}} = \int_{\Omega} G_i u^{*}_i\,\mathrm{d}v + \int_{\partial\Omega} \left(t_i u^{*}_i + T_{ij} f^{*}_{ij}\right) \mathrm{d}s$$

- The virtual work equations can be extended to large strain problems

Numerical Approach

Second gradient model formulation: strong form

$$\begin{cases} \dfrac{\partial(\boxed{\sigma_{ij}} - \boxed{\tau_{ij}})}{\partial x_j} + G_i = 0 \\[2ex] \dfrac{\partial \boxed{\chi_{ijk}}}{\partial x_k} - \tau_{ij} = 0 \end{cases}$$

$$\begin{cases} (\sigma_{ij} - \tau_{ij})n_j = t_i \\[2ex] \chi_{ijk} n_k = T_{ij} \end{cases}$$

Three constitutive equations needed !

Numerical Approach

Local Second gradient model formulation:

- Addition of a kinematical constraint (Chambon et al., 1998; Matsushima et al., 2002)

$$f_{ij} = F_{ij}$$

this implies:

$$f_{ij} = \frac{\partial u_i}{\partial x_j}$$

the virtual work equation reads

$$\int_{\Omega} \left(\sigma_{ij} D^*_{ij} + \chi_{ijk} \frac{\partial^2 u^*_i}{\partial x_j \partial x_k} \right) \mathrm{d}v = \int_{\Omega} G_i u^*_i \, \mathrm{d}v + \int_{\partial\Omega} \left(p_i u^*_i + P_i D u^*_i \right) \mathrm{d}s$$

Numerical Approach

<u>Local</u> **Second gradient model formulation: strong form**

$$\frac{\partial \sigma_{ij}}{\partial x_j} - \frac{\partial^2 \chi_{ijk}}{\partial x_j \partial x_k} + G_i = 0$$

$$\boxed{\sigma_{ij} n_j} - \boxed{n_k n_j D\chi_{ijk} - \frac{D\chi_{ijk}}{Dx_k} n_j - \frac{D\chi_{ijk}}{Dx_j} n_k + \frac{Dn_l}{Dx_l} \chi_{ijk} n_j n_k - \frac{Dn_j}{Dx_k} \chi_{ijk}} = p_i$$

$$\chi_{ijk} n_j n_k = P_i$$

Numerical Approach

<u>Local</u> Second gradient model formulation: weak form

$$\int_{\Omega}\left(\sigma_{ij}\frac{\partial u_i^*}{\partial x_j}+\Sigma_{ijk}\frac{\partial^2 u_i^*}{\partial x_j \partial x_k}\right)d\Omega = W_{ext}^*$$

Local quantities

Introduction of Lagrange multiplier field :

$$\int_{\Omega}\left(\sigma_{ij}\frac{\partial u_i^*}{\partial x_j}+\Sigma_{ijk}\frac{\partial v_{ij}^*}{\partial x_k}\right)d\Omega - \int_{\Omega}\lambda_{ij}\left(\frac{\partial u_i^*}{\partial x_j}-v_{ij}^*\right)d\Omega = W_{ext}^*$$

$$\int_{\Omega}\lambda_{ij}^*\left(\frac{\partial u_i}{\partial x_j}-v_{ij}\right)d\Omega = 0$$

Numerical Approach

Local Second gradient model formulation: weak form

Local Second gradient Finite element

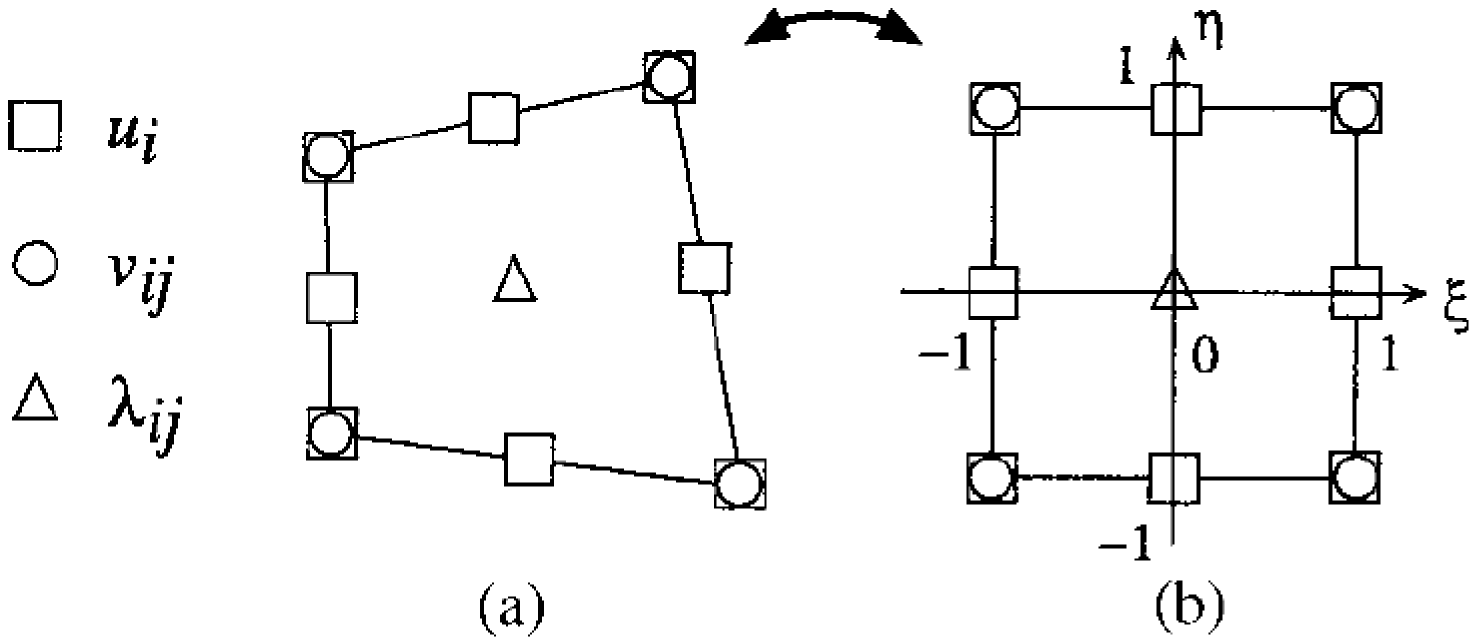

Numerical Approach

LIÈGE université
Urban & Environmental Engineering

Example n°1: Biaxial test (again)

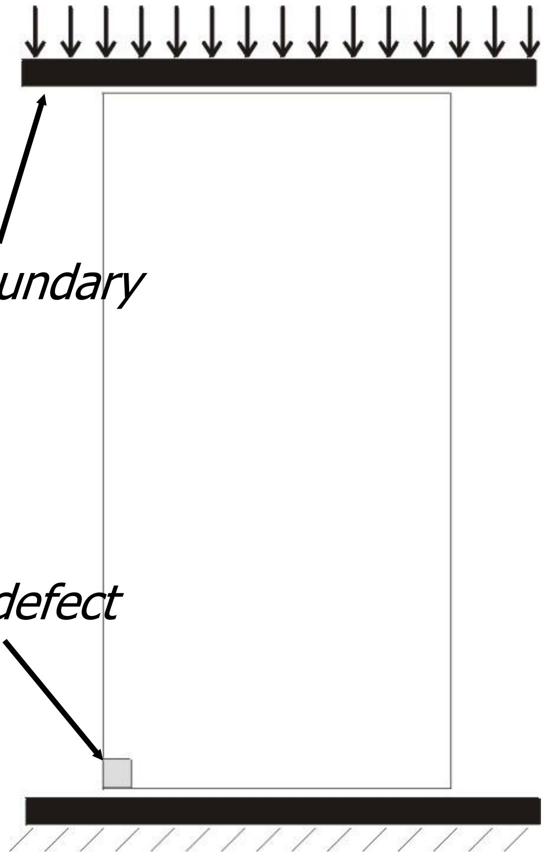

Strain rate : 0.18% / hour

No lateral confinement

Globally drained (upper and lower drainage)

Numerical Approach

Example n°1: Biaxial test (again)

First gradient law

Linear elasticity : E_0 *et* ν_0

Drucker Prager criterion : $$F \equiv \sqrt{\frac{3}{2}} II_{\hat{\sigma}} + m\left(I_\sigma - \frac{3c}{\tan\phi} \right) = 0$$

$$m = \frac{2\sin\phi}{3-\sin\phi} \qquad c = c_0\, f(\gamma^p)$$

Associated softening plasticity (decrease of cohesion) :

$$f(\gamma^p) = \left(1 - (1-\alpha)\frac{\gamma^p}{\gamma_R^p} \right)^2 \; si \; 0 < \gamma^p < \gamma_R^p$$
$$= \alpha^2 \; si \; \gamma^p \geq \gamma_R^p$$

Numerical Approach

Example n°1: Biaxial test (again)

- *Second gradient law :* *Linear relationship deduced from Mindlin*

$$
\begin{bmatrix} \tilde{\Sigma}_{111} \\ \tilde{\Sigma}_{112} \\ \tilde{\Sigma}_{121} \\ \tilde{\Sigma}_{122} \\ \tilde{\Sigma}_{211} \\ \tilde{\Sigma}_{212} \\ \tilde{\Sigma}_{221} \\ \tilde{\Sigma}_{222} \end{bmatrix}
=
\begin{bmatrix}
D & 0 & 0 & 0 & 0 & \frac{D}{2} & \frac{D}{2} & 0 \\
0 & \frac{D}{2} & \frac{D}{2} & 0 & -\frac{D}{2} & 0 & 0 & \frac{D}{2} \\
0 & \frac{D}{2} & \frac{D}{2} & 0 & -\frac{D}{2} & 0 & 0 & \frac{D}{2} \\
0 & 0 & 0 & D & 0 & -\frac{D}{2} & -\frac{D}{2} & 0 \\
0 & -\frac{D}{2} & -\frac{D}{2} & 0 & D & 0 & 0 & 0 \\
\frac{D}{2} & 0 & 0 & -\frac{D}{2} & 0 & \frac{D}{2} & \frac{D}{2} & 0 \\
\frac{D}{2} & 0 & 0 & -\frac{D}{2} & 0 & \frac{D}{2} & \frac{D}{2} & 0 \\
0 & \frac{D}{2} & \frac{D}{2} & 0 & 0 & 0 & 0 & 0
\end{bmatrix}
\begin{bmatrix} \frac{\partial \dot{v}_{11}}{\partial x_1} \\ \frac{\partial \dot{v}_{11}}{\partial x_2} \\ \frac{\partial \dot{v}_{12}}{\partial x_1} \\ \frac{\partial \dot{v}_{12}}{\partial x_2} \\ \frac{\partial \dot{v}_{21}}{\partial x_1} \\ \frac{\partial \dot{v}_{21}}{\partial x_2} \\ \frac{\partial \dot{v}_{22}}{\partial x_1} \\ \frac{\partial \dot{v}_{22}}{\partial x_2} \end{bmatrix}
$$

D = 20 kN

Numerical Approach

Example n°1: Biaxial test (again)

Bifurcation directions

(Regularization : Second gradient)

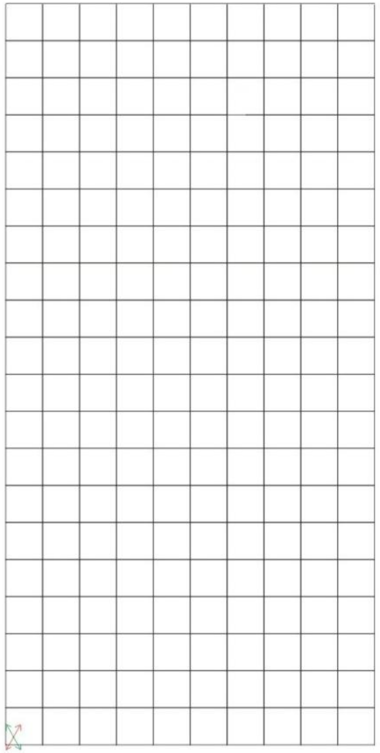

Before

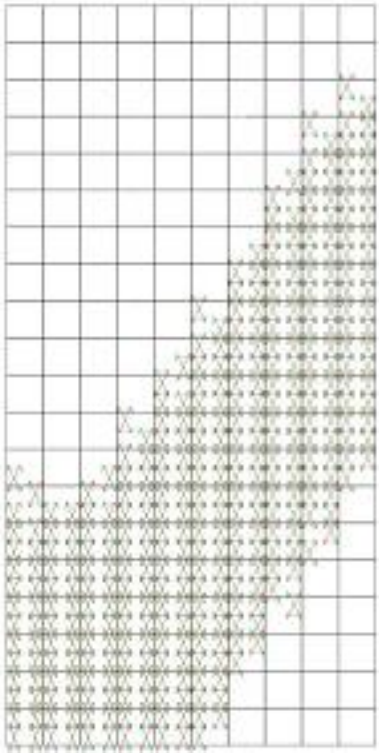

After

Numerical Approach

Example n°1: Biaxial test (again)

Plastic loading point

(Regularization : Second gradient)

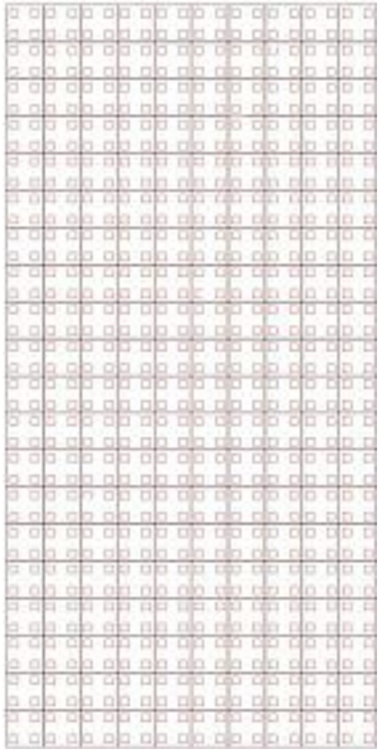

Before

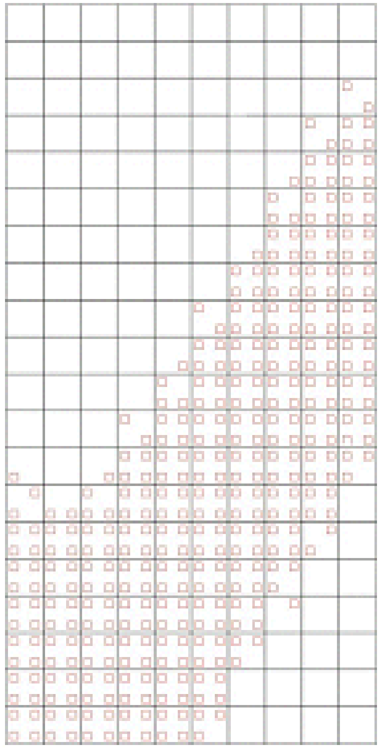

After

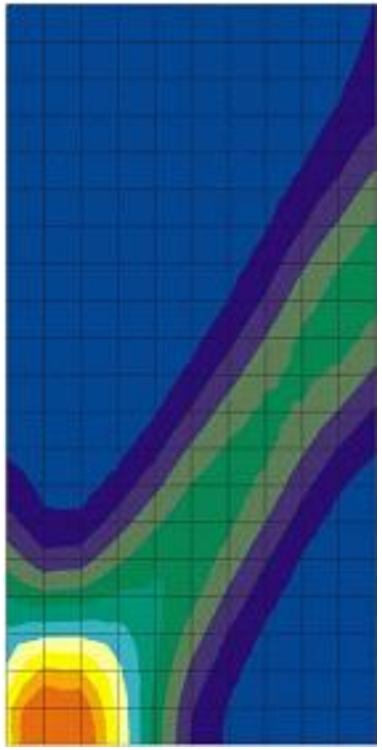

Numerical Approach

Example n°1: Biaxial test (again)

Velocity field

(Regularization : Second gradient)

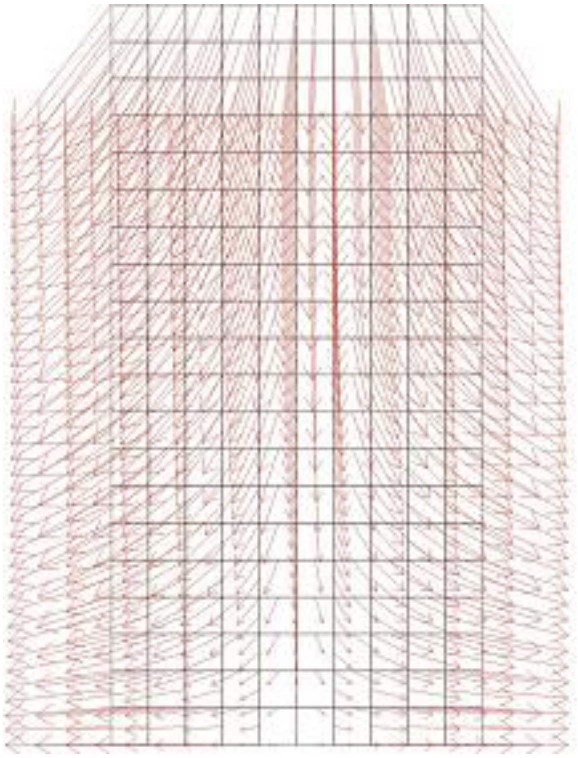

Before

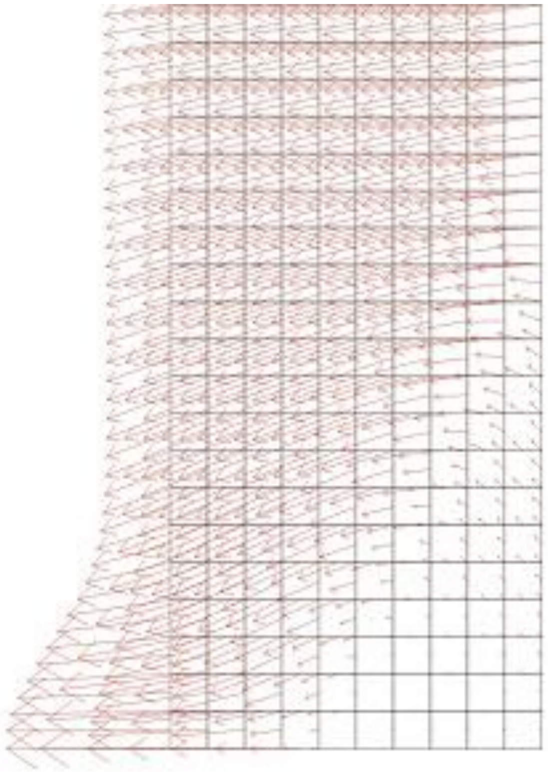

After

Numerical Approach

Example n°1: Biaxial test (again)

Initiation of localization (Directional research – Chambon et al., 2001)

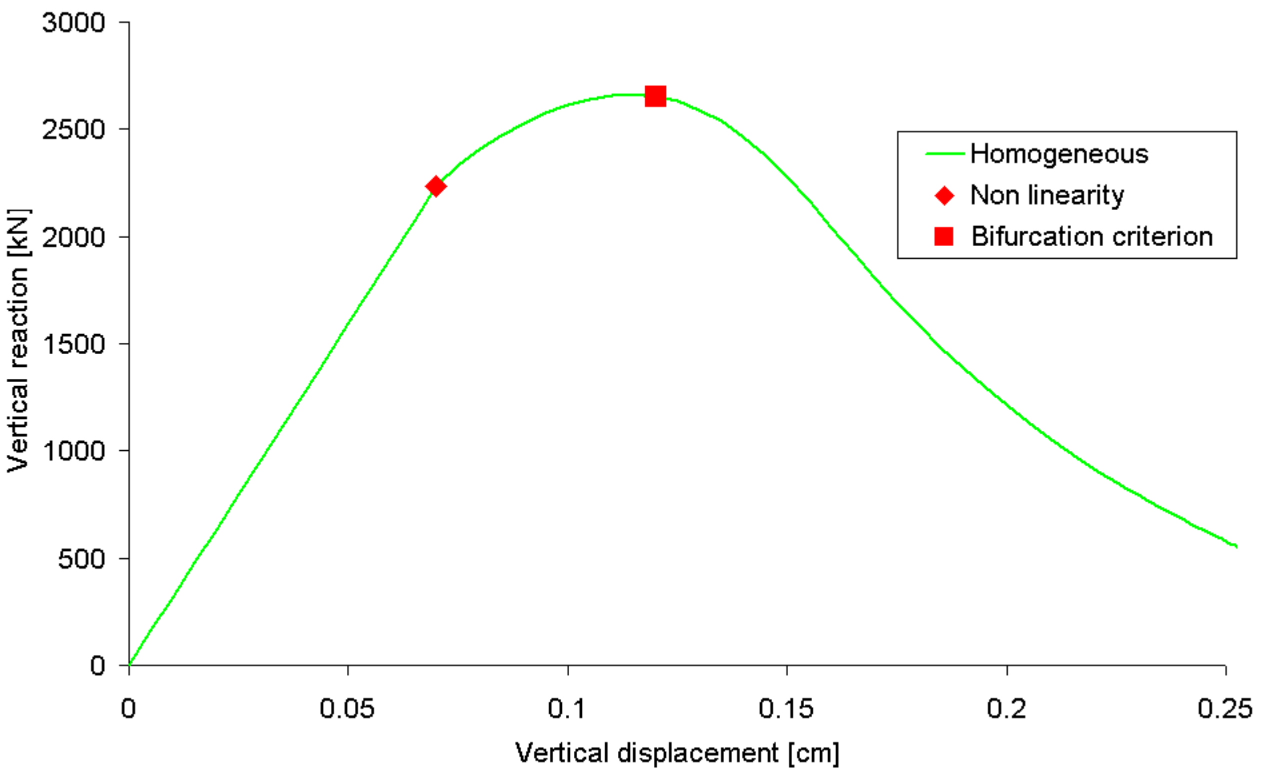

Numerical Approach

Example n°1: Biaxial test (again)

Initiation of localization (Directional research)

(Regularization : Second gradient)

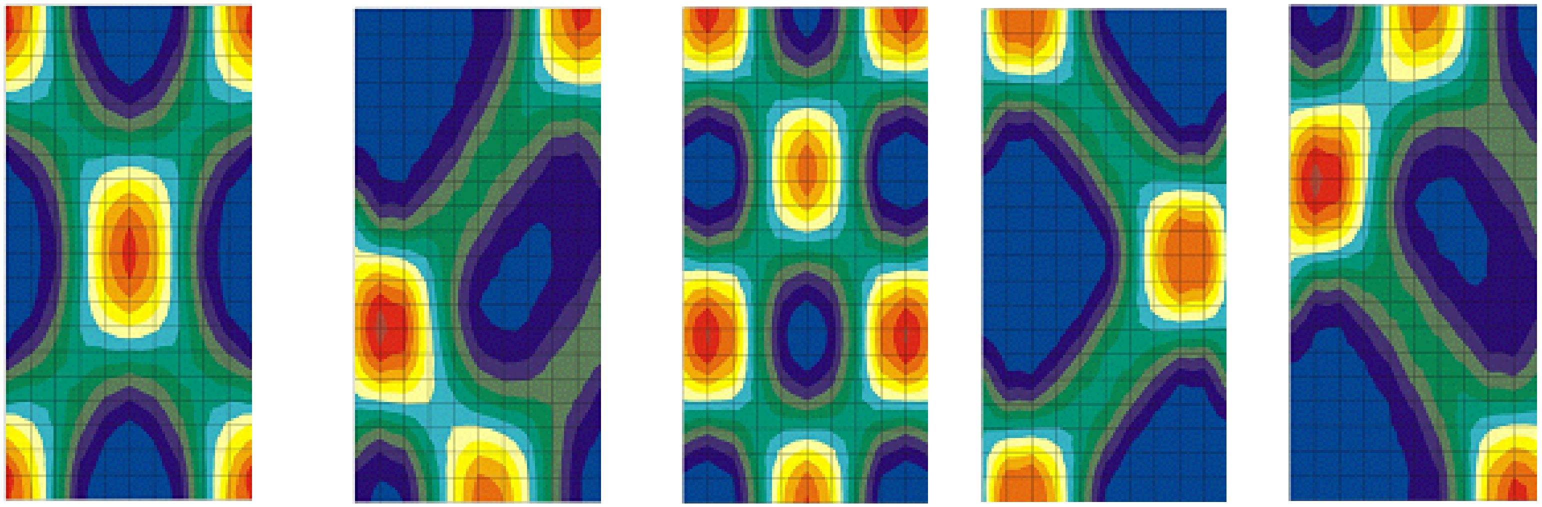

Non uniqueness of the solution

Numerical Approach

Example n°1: Biaxial test (again)

Initiation of localization (Directional research)

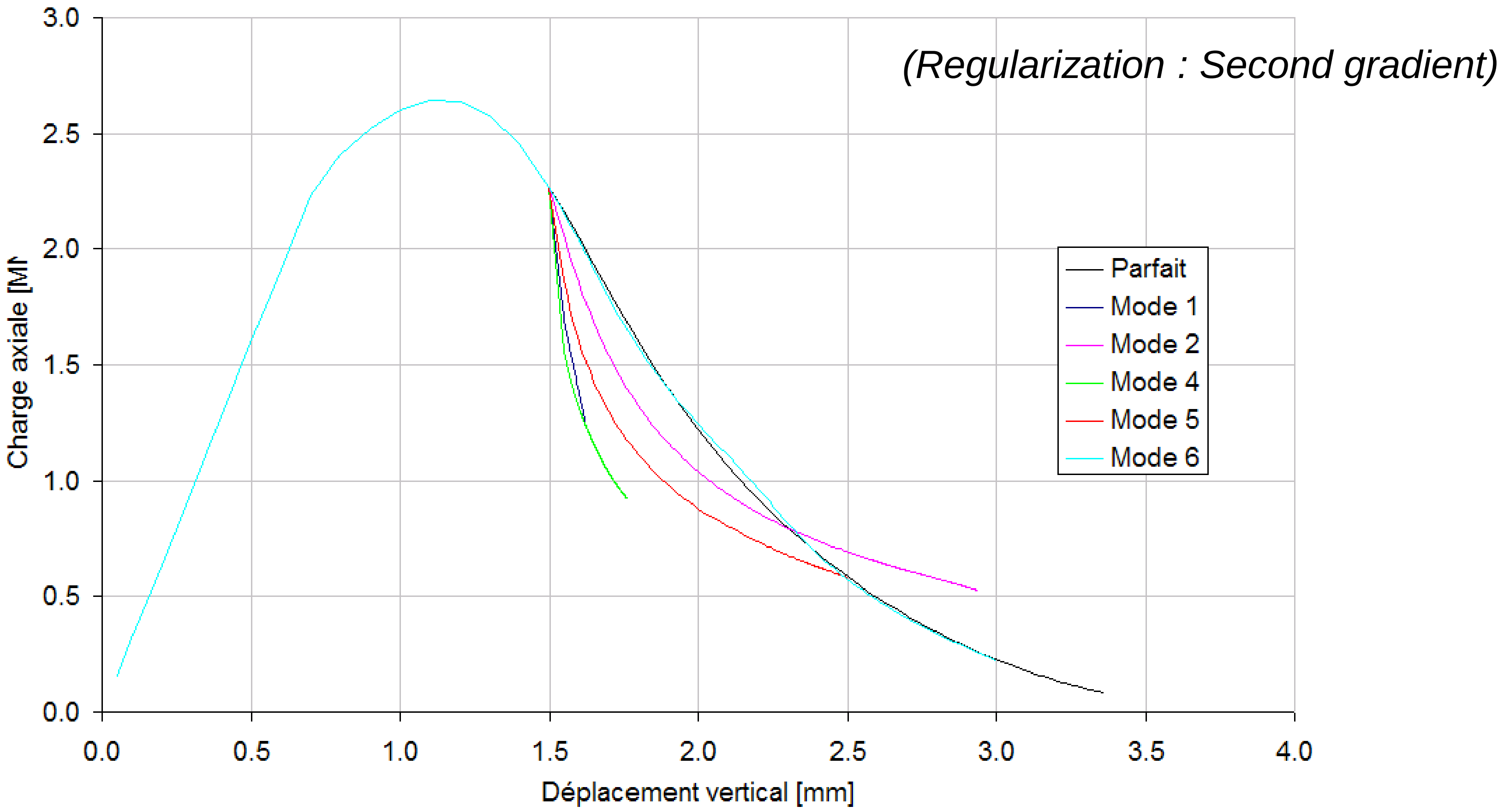

Non uniqueness of the solution

Numerical Approach

LIÈGE université
Urban & Environmental Engineering

Example n°1: Biaxial test (again)

Localization mode switching (Bésuelle et al.,2006)

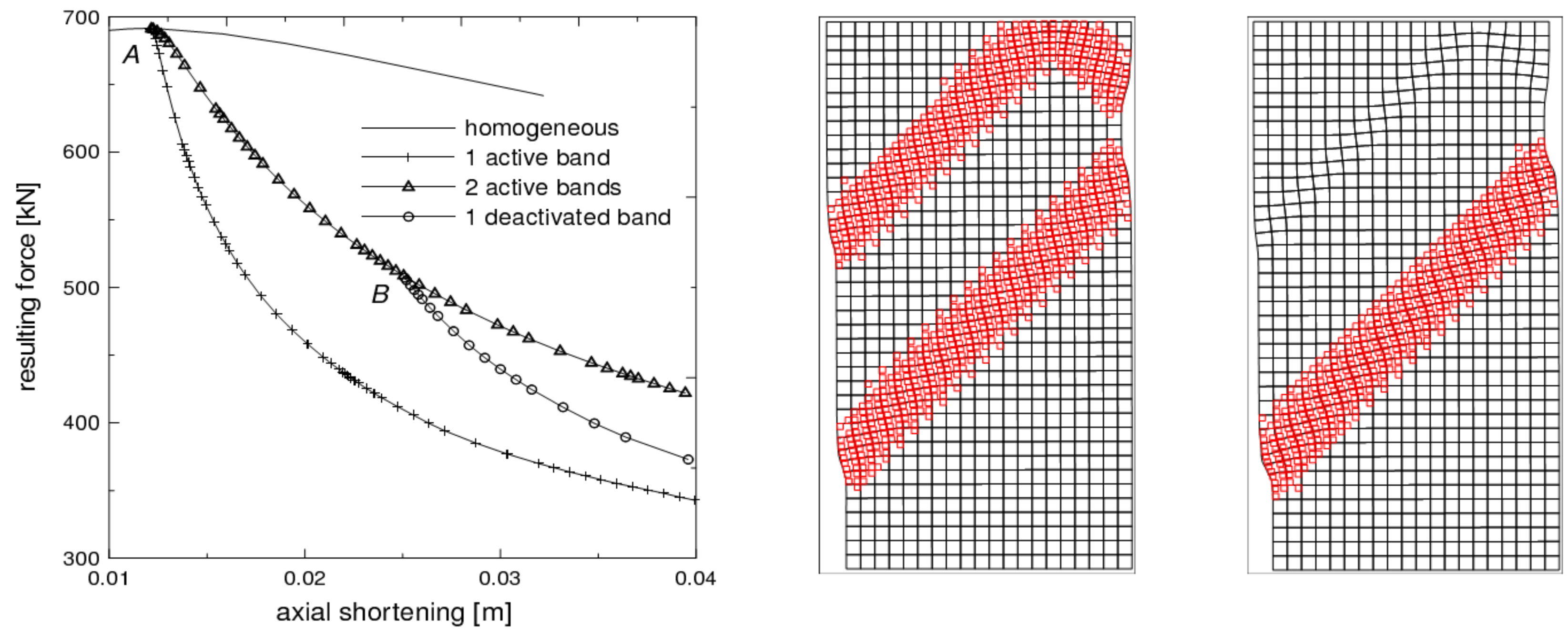

Non uniqueness of the solution

Numerical Approach

Local Second gradient HM model formulation: weak form

- ✓ Second gradient effects are assumed only for solid phase
- ✓ For the mixture, there are stresses which obey the Terzaghi postulate and double stresses which are only the one of the solid phase
- ✓ Boundary conditions for the mixture are enriched

Numerical Approach

<u>Local</u> Second gradient <u>HM</u> model formulation: weak form

$$\int_{\Omega}\left(\sigma_{ij}\frac{\partial u_i^*}{\partial x_j}+\Sigma_{ijk}\frac{\partial^2 u_i^*}{\partial x_j \partial x_k}\right)d\Omega = W_{ext}^*$$

$$\int_{\Omega}\dot{M}\,p^* - m_i\frac{\partial p^*}{\partial x_i}d\Omega = \int_{\Omega}Q\,p^* d\Omega + \int_{\Gamma}\bar{q}\,p^* d\Gamma$$

Darcy's law $$m_i = -\rho_w\frac{\kappa}{\mu}\left(\frac{\partial p}{\partial x_i}+\rho_w g_i\right)$$

Storage law $$\dot{M} = \rho_w\frac{\dot{p}}{k^w}\phi + \rho_w\frac{\dot{\Omega}}{\Omega}$$

Numerical Approach

<u>Local</u> Second gradient <u>HM</u> model formulation:

Isoparametric Finite Element :

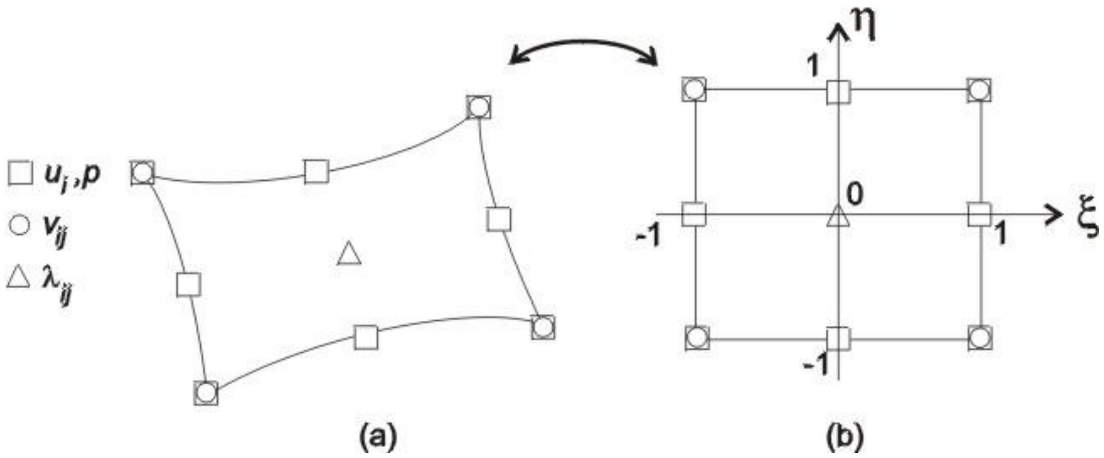

8 nodes for macro-displacement and pressure field
4 nodes for microkinetic gradient field
1 node for Lagrange multipliers field

Numerical Approach

Example n°1: Biaxial test (last time)

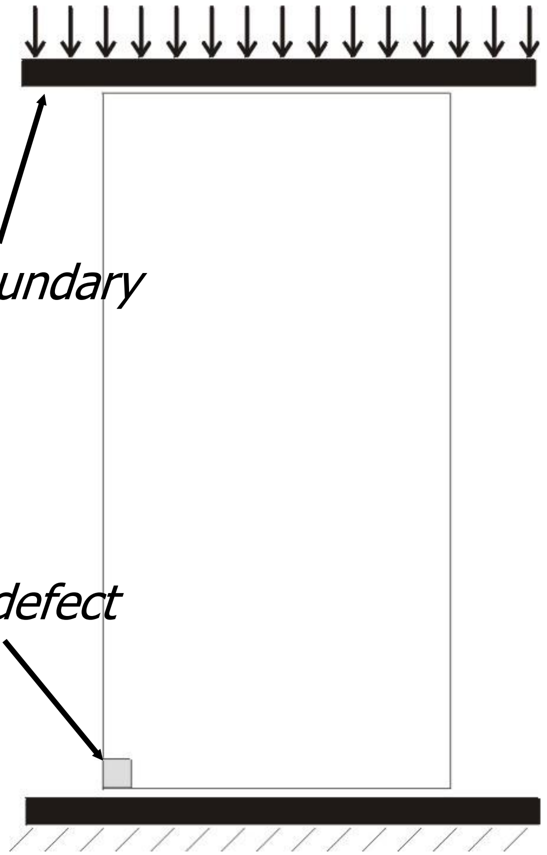

Strain rate : 0.18% / hour

No lateral confinement

Globally drained (upper and lower drainage)

Numerical Approach

- *Equivalent strain after 0.2 % of axial strain (κ = 10^{-12} m²)*

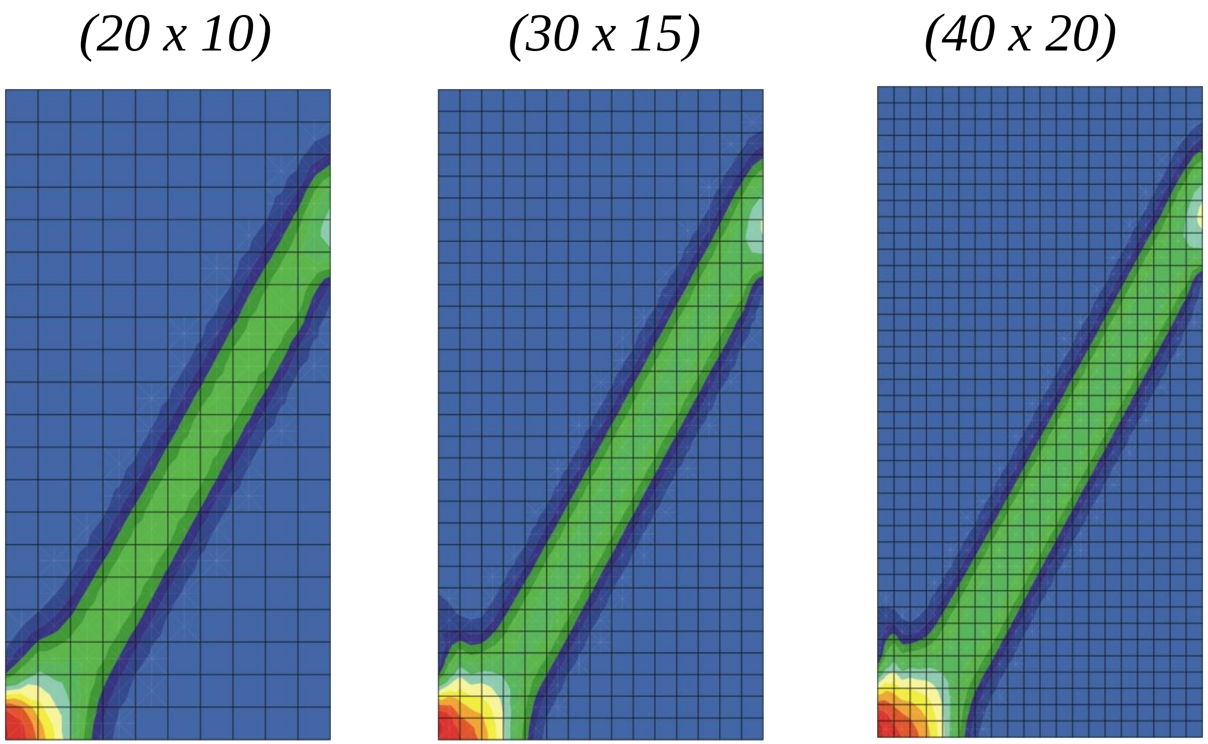

Numerical Approach

- *Plastic loading point after 0.2 % of axial strain ($\kappa = 10^{-12}$ m²)*

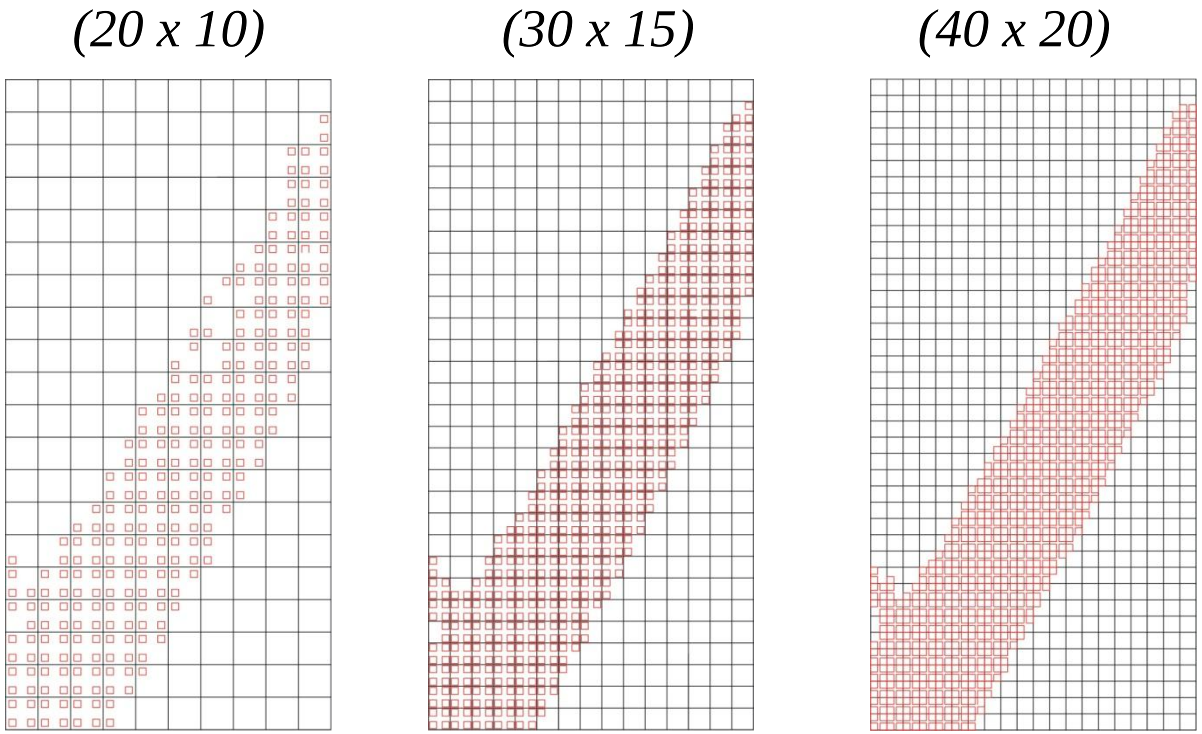

Numerical Approach

Coupled modelling – Comparison Coarse mesh - Refined mesh

Coupled second gradient FE formulation

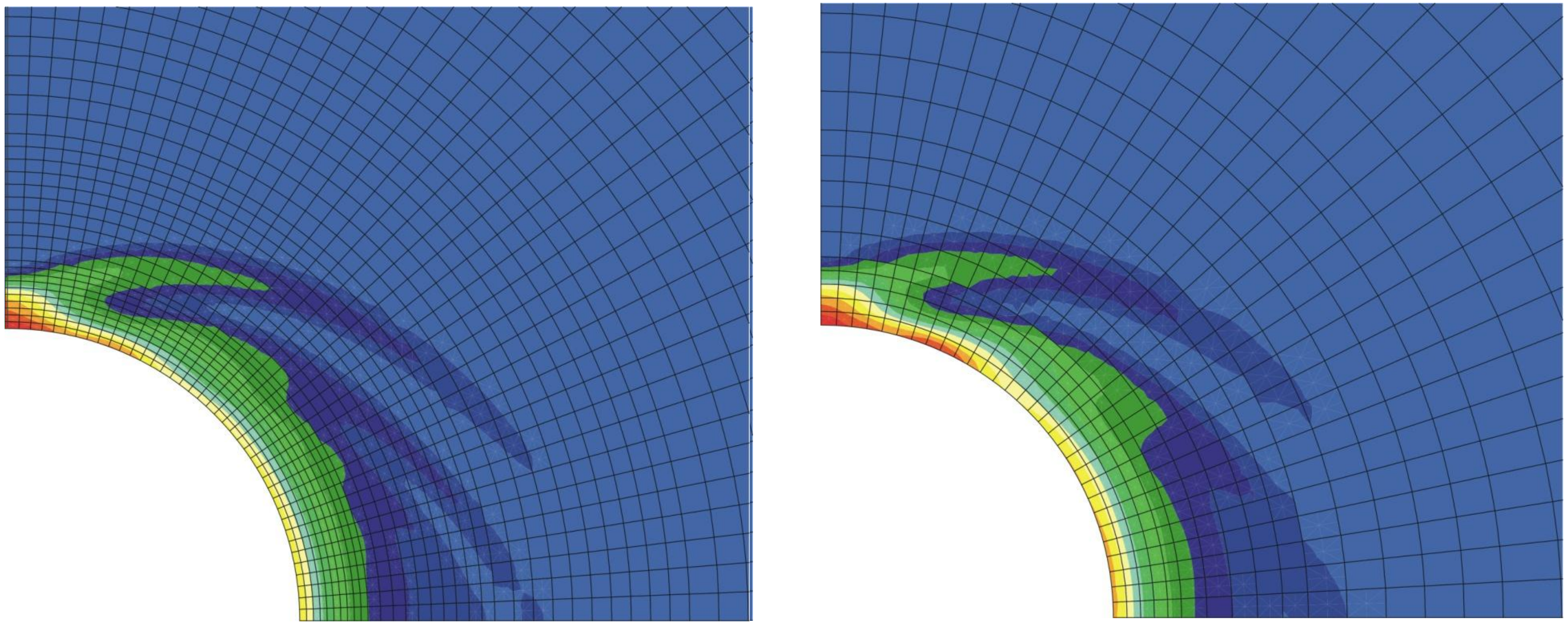

Deviatoric strains

Table of Contents

LIÈGE université
Urban & Environmental Engineering

Context

Rupture accross the scale

Theoretical Approach

Localized mode of deformation

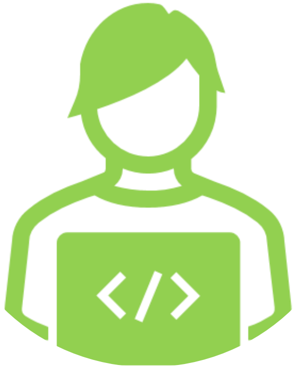

Numerical Approach

Second gradient model

Application

Underground nuclear waste disposal

Long term management of radioactive wastes

Intermediate
(long-lived)
&
high activity
wastes

Deep geological disposal

Repository in deep geological media with good confining properties

(Low permeability $K<10^{-12}$ m/s)

Underground structures

= network of galleries

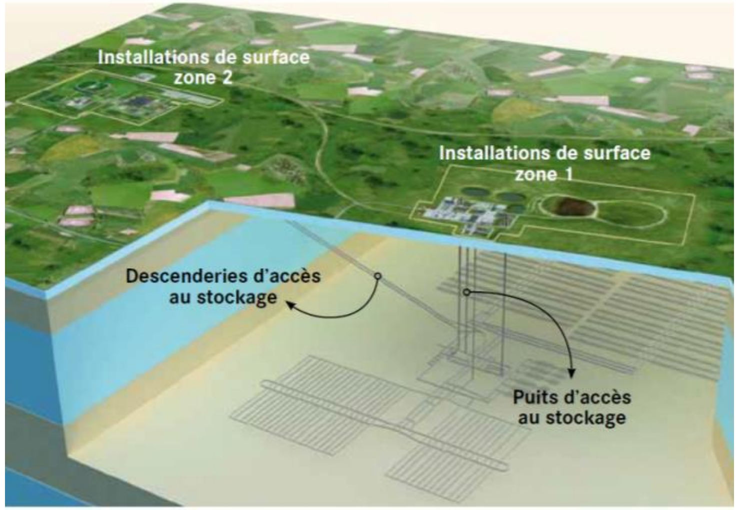

Long term management of radioactive wastes

<u>Callovo-Oxfordian claystone (COx)</u>

Sedimentary clay rock (France).

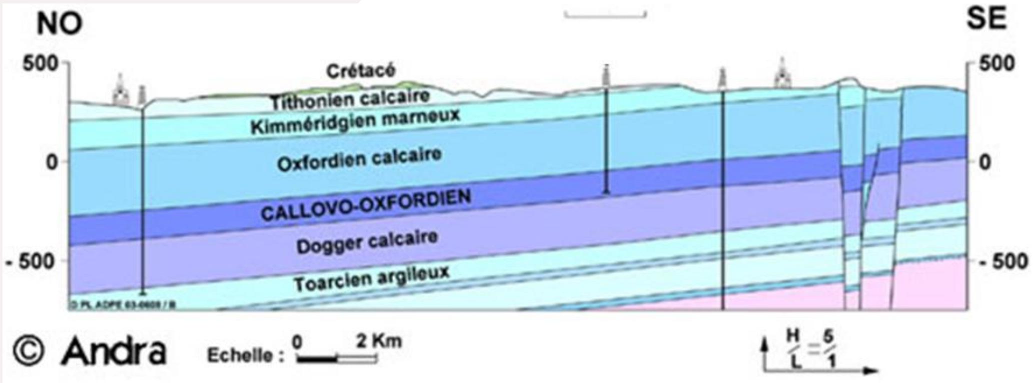

Borehole core samples
(Andra, 2005)

- <u>Underground research laboratory</u>

Feasibility of a safe repository

France (Meuse / Haute-Marne, Bure)

(Armand et al., 2014)

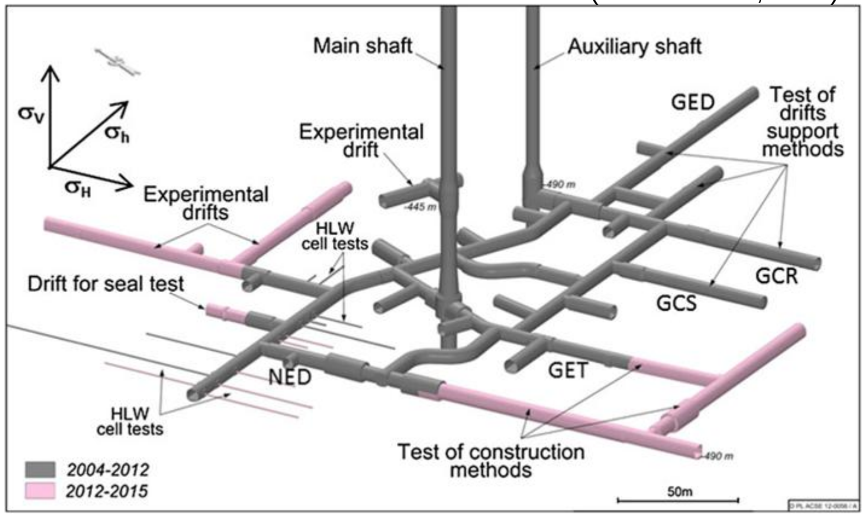

Repository phases

Time

Construction
→ Excavation

Maintenance
→ Ventilation

Repository
→ Sealing

Long term
→ Corrosion,
heat generation

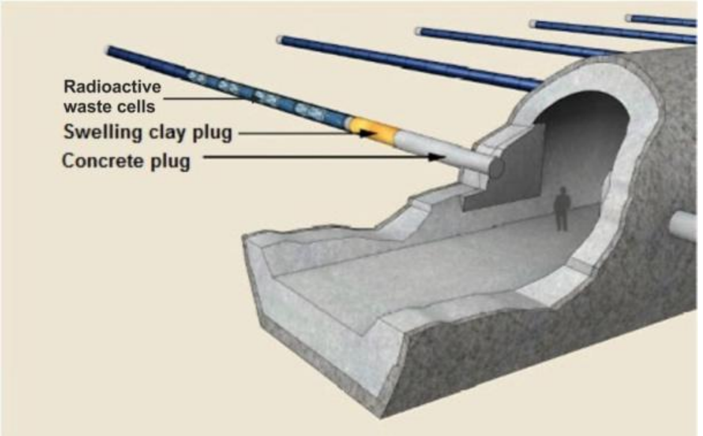

Type C wastes (Andra, 2005)

THM COUPLINGS

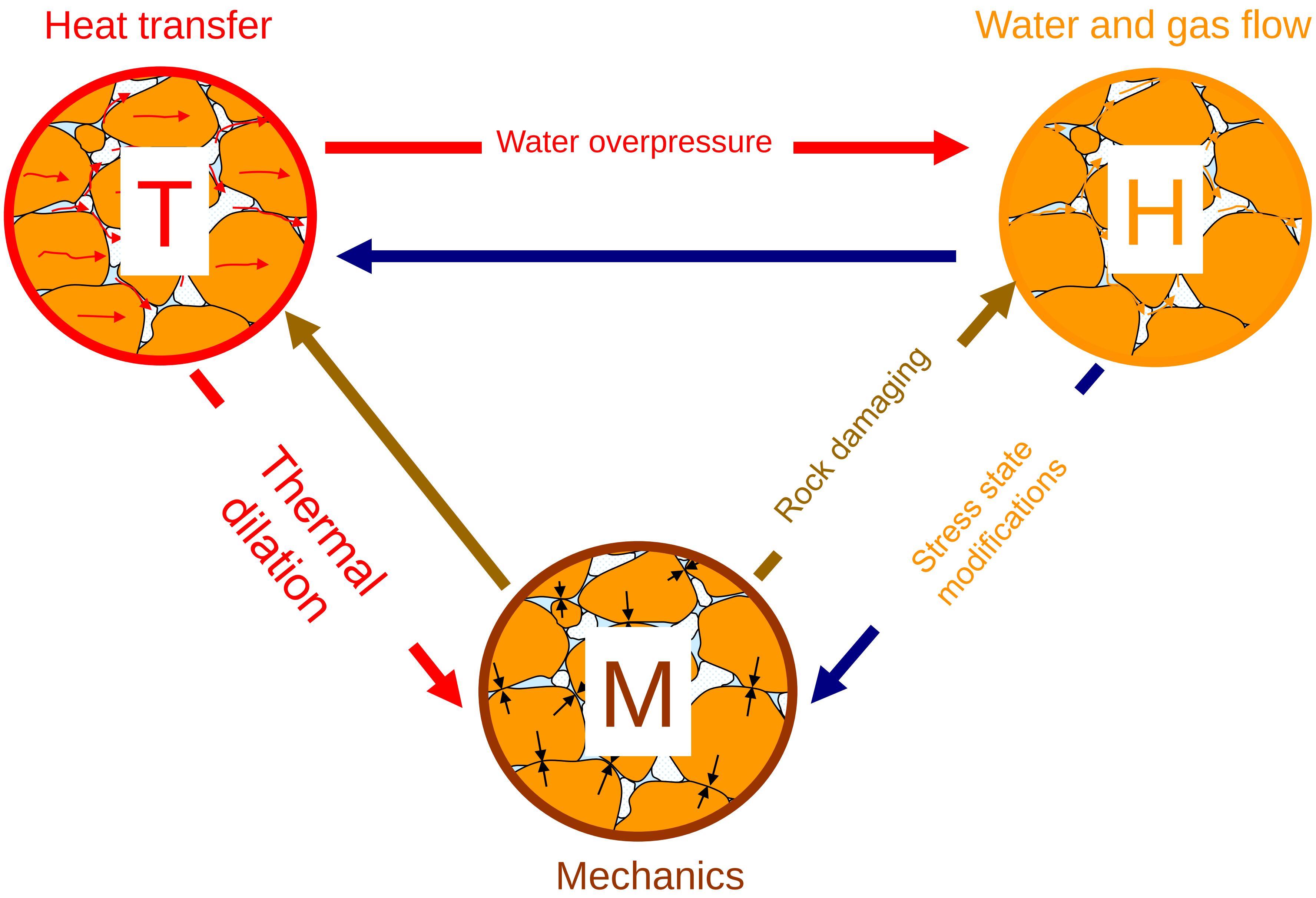

Repository phases

Time

Construction

Excavation

Maintenance

Ventilation

Repository

Sealing

Long term

Corrosion,
heat generation

Type C wastes (Andra, 2005)

Excavated damaged zone - EDZ

Construction Mechanical fracturing
Excavation
↓
Stress redistribution
↓
Damage / Fracturing
↓
Coupled processes HM property modifications
↓
Safety function alteration

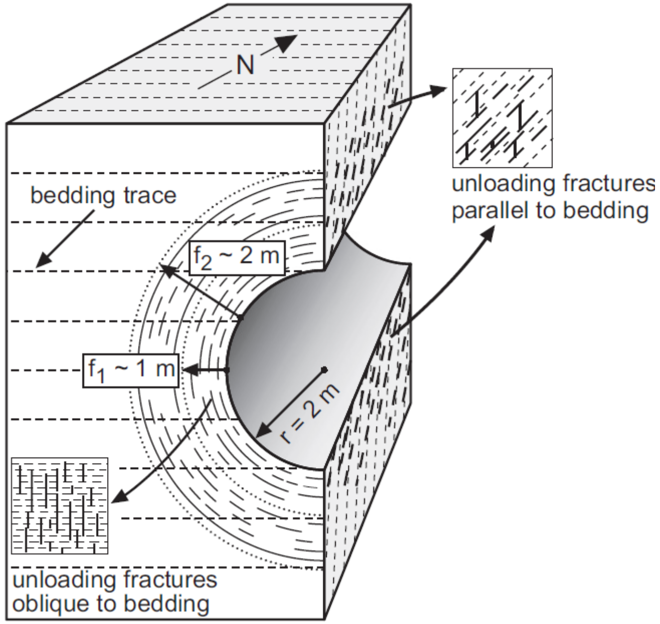

Fracturing & permeability increase
(several orders of magnitude)

Opalinus clay in Switzerland
(Bossart et al., 2002)

Maintenance Water transfer
Galleries ventilation
↓
Air-rock interaction
↓
Drainage / desaturation
↓
Modification of the water transfer

Fracturation observation

Anisotropies: - stress : $\sigma_H > \sigma_h \sim \sigma_v$

- material : HM cross-anisotropy.

(Armand et al., 2014)

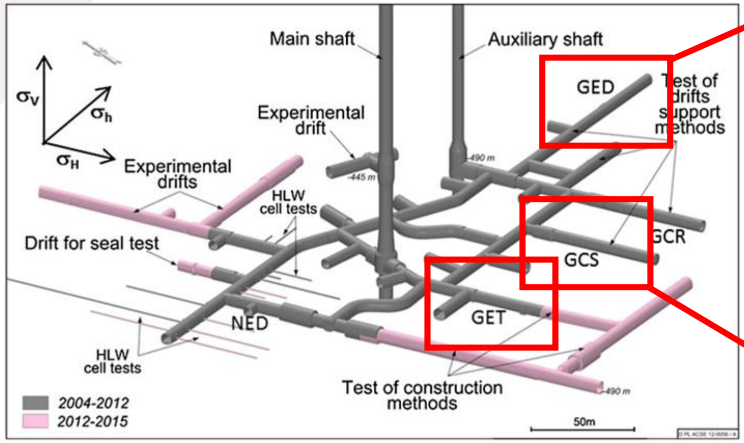

Galery // to σ_h

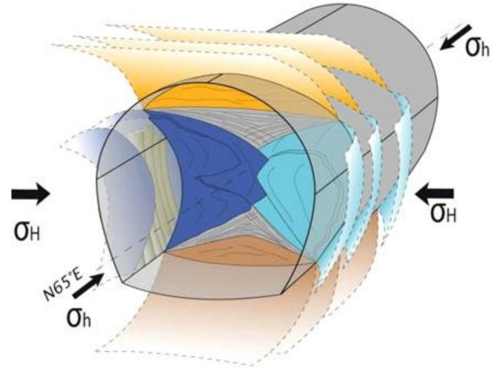

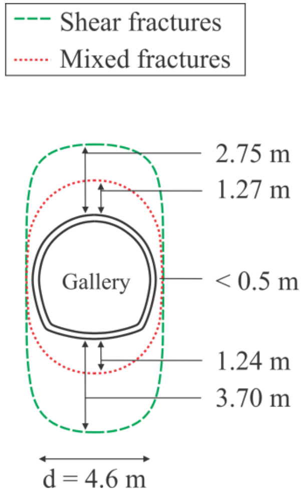

Galery // to σ_H

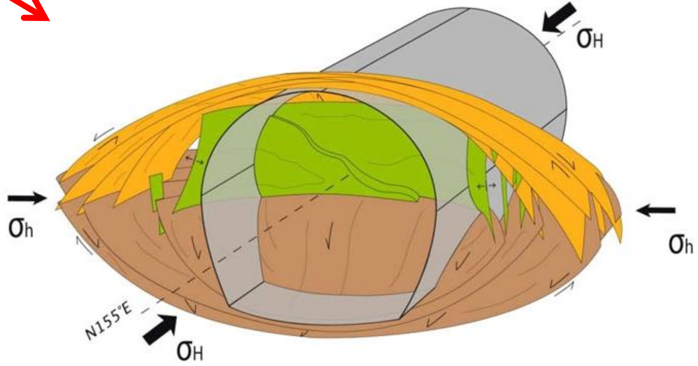

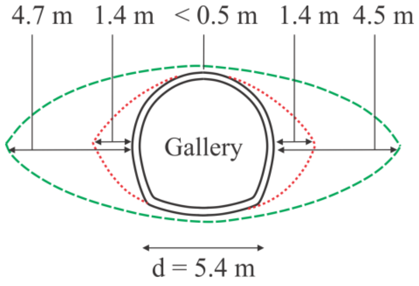

Issues: Prediction of the fracturing.
Effect of anisotropies ?
Permeability evolution & relation to fractures ?

Excavation / Fracturation modelling

LIÈGE université
Urban & Environmental Engineering

Constitutive models for COx

- Mechanical law - 1st gradient model

Isotropic elasto-plastic internal friction model

Non-associated plasticity, Van Eeckelen yield surface :

$$F \equiv II_{\hat{\sigma}} - m\left(I_{\sigma'} + \frac{3\,c}{\tan\varphi_C}\right) = 0$$

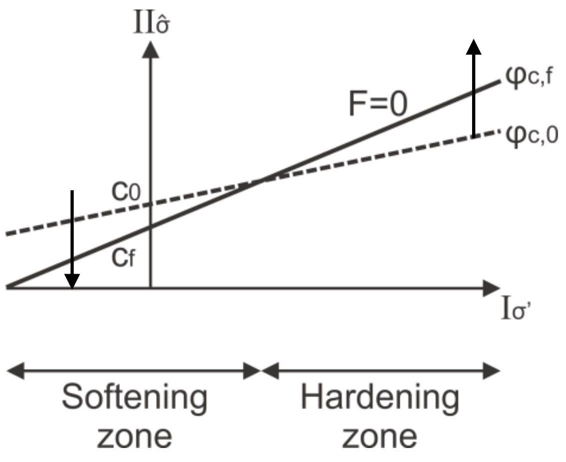

φ hardening / c softening

$$c = c_0 + \frac{\left(c_f - c_0\right)\hat{\varepsilon}^p_{eq}}{B_c + \hat{\varepsilon}^p_{eq}}$$

→ Strain localisation

- Hydraulic law

Fluid mass flow (advection, Darcy) : $$f_{w,i} = -\rho_w \frac{k_{w,ij}\,k_{r,w}}{\mu_w}\left(\frac{\partial p_w}{\partial x_j} + \rho_w\, g_j\right)$$

Water retention and permeability curves (Mualem - Van Genuchten's model)

Excavation / Fracturation modelling

- Numerical model

HM modelling in 2D plane strain state

Gallery radius = 2.3 m

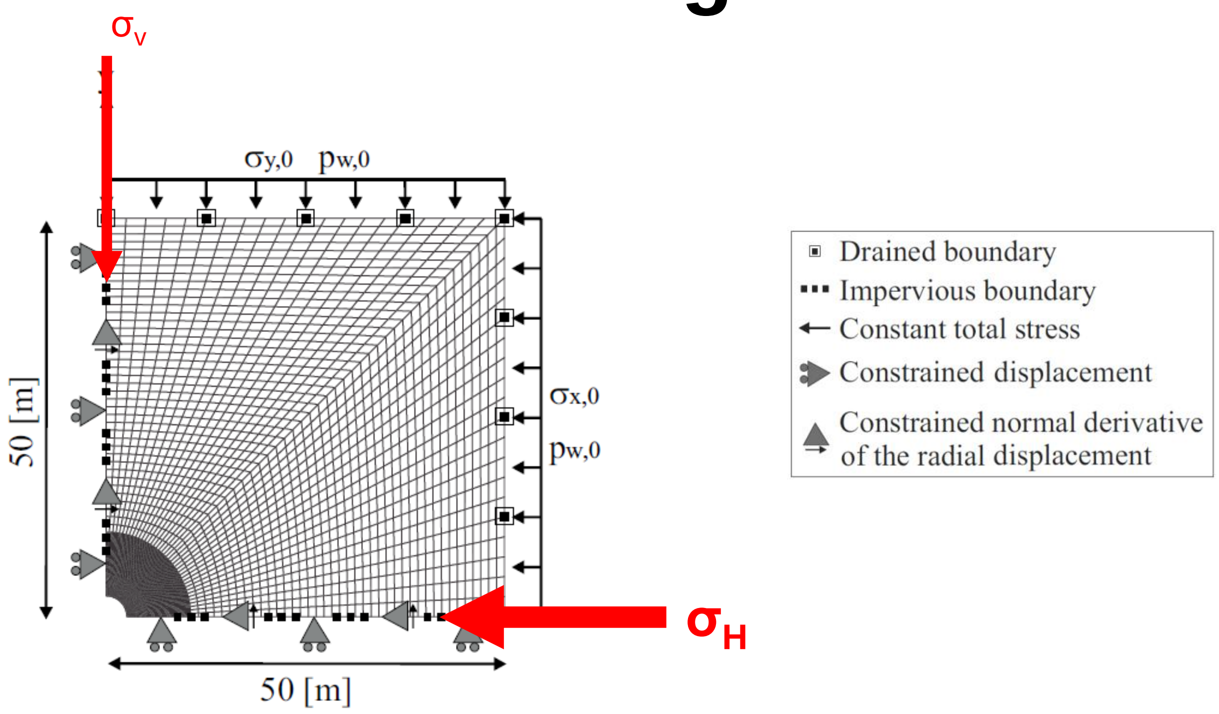

- Gallery in COx // σ_h

Effect of stress anisotropy

Anisotropic stress state

$p_{w,0}$ = 4.5 [MPa]

$\sigma_{x,0} = \sigma_H = 1.3\ \sigma_v$ = 15.6 [MPa]

$\sigma_{y,0} = \sigma_v$ = 12 [MPa]

$\sigma_{z,0} = \sigma_h$ = 12 [MPa]

- Excavation

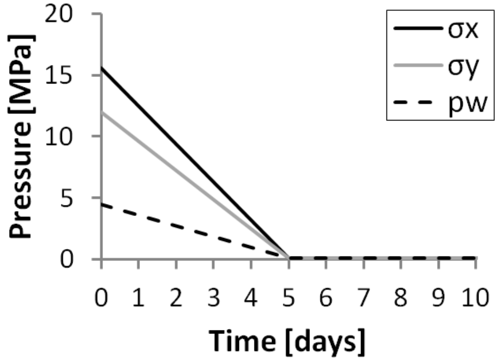

Excavation / Fracturation modelling

- Localisation zone

Incompressible solid grains, b=1

1009 days

End of excavation

Total deviatoric strain

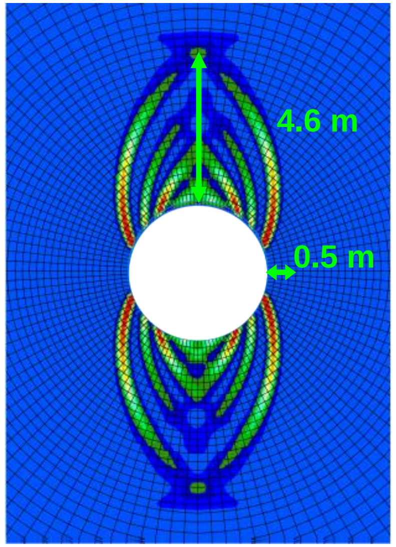

$$\hat{\varepsilon}_{eq} = \sqrt{\frac{2}{3}\hat{\varepsilon}_{ij}\hat{\varepsilon}_{ij}}$$

0 0.06

Plasticity

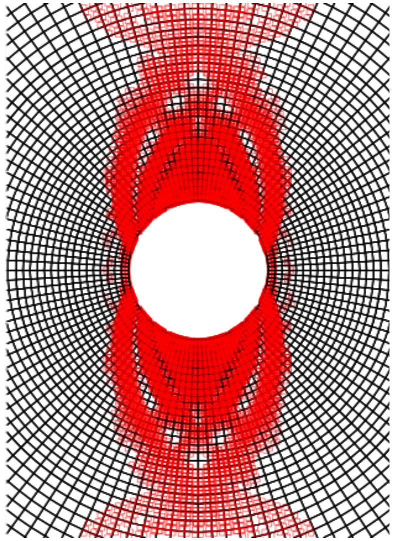

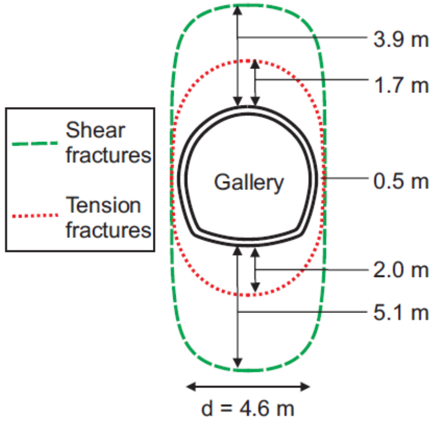

→ For an isotropic mechanical behaviour, the appearance and shape of the strain localisation are mainly due to mechanical effects linked to the anisotropic stress state.

Excavation / Fracturation modelling

- Convergence:

Important during the excavation
Anisotropic convergence
Influence of the ventilation
Experimental results (GED - Andra’s URL)
No strain localisation

Calcul
She
Sh

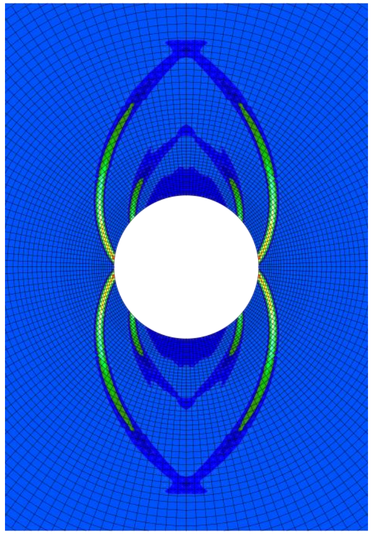

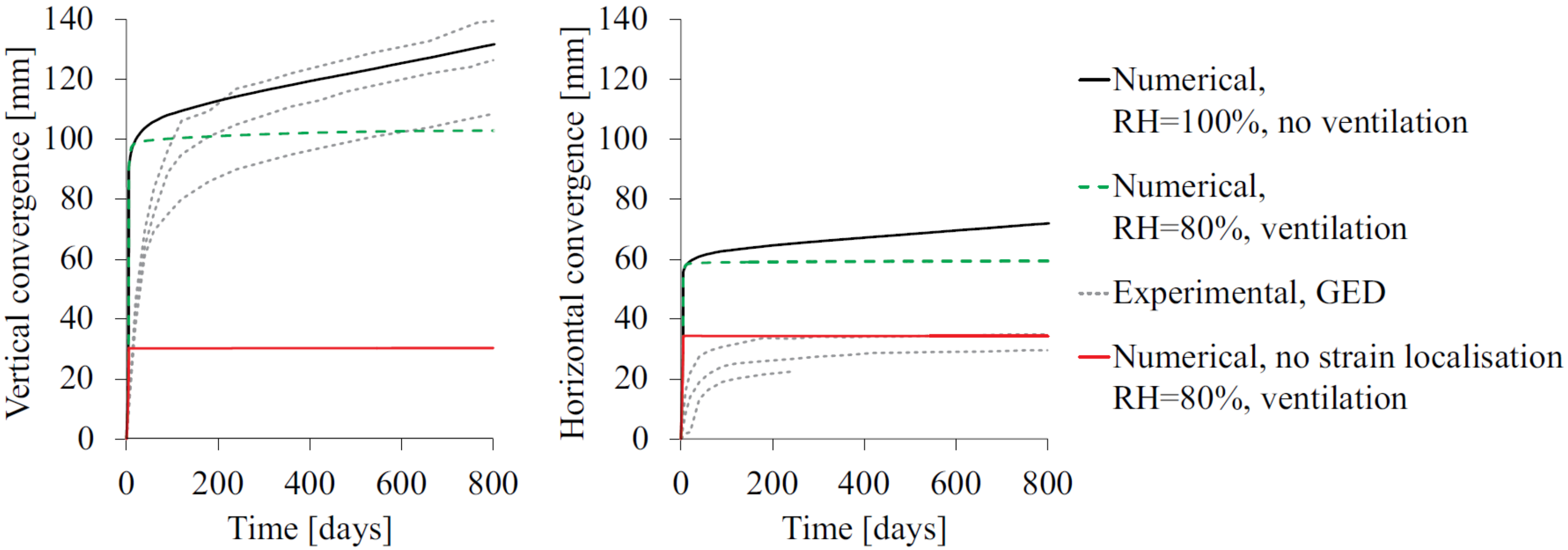

Excavation / Fracturation modelling

Conclusions and outlooks

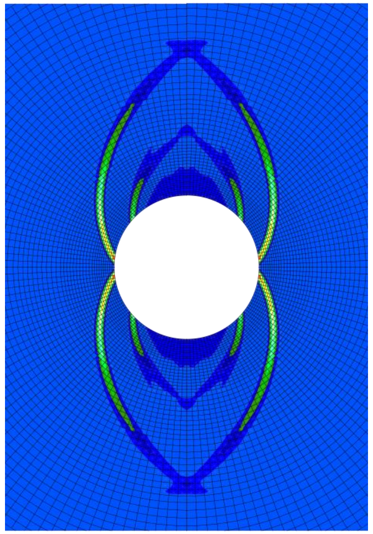

✓ Reproduction of EDZ with shear bands.

✓ Shape and extent of EDZ **governed by anisotropic stress state.**

- Next steps …

X Mechanical rock behaviour.

→ Material anisotropy, gallery // σ_H .

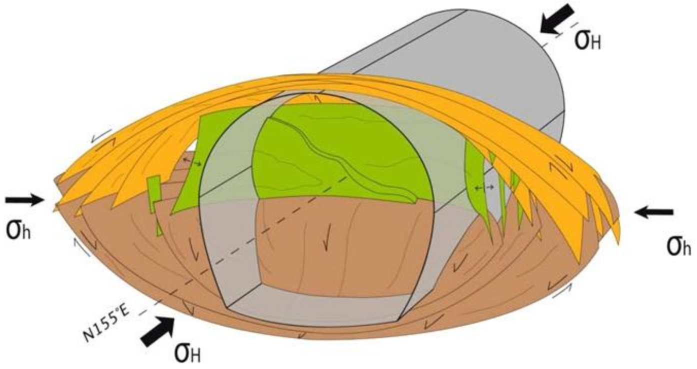

Excavation / Fracturation modelling

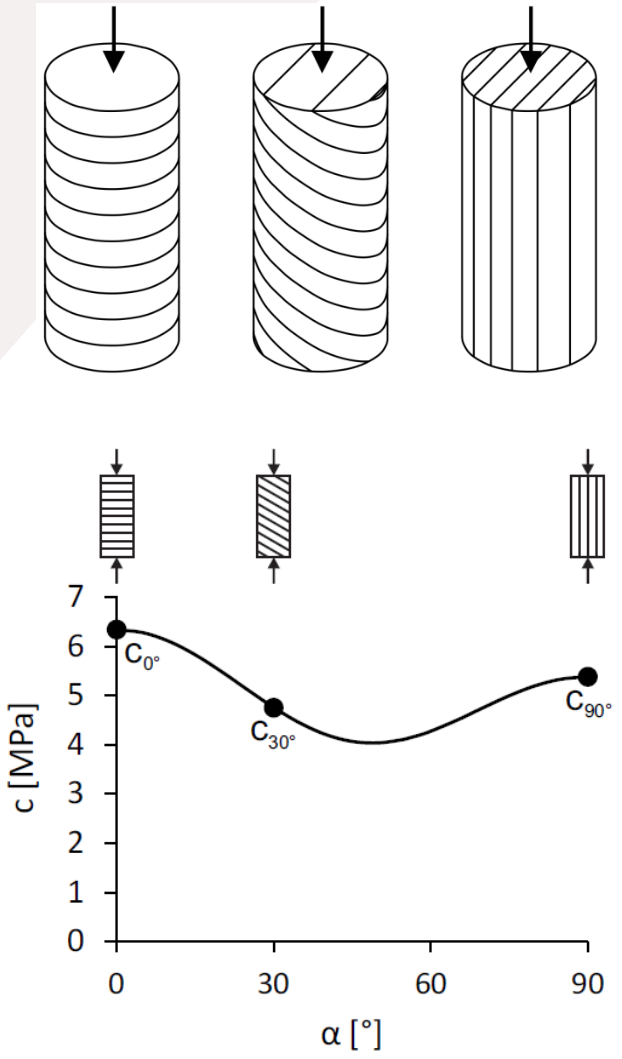

- Linear elasticity :

Cross-anisotropic (5 param.) + Biot's coefficients

$$E_{//}, E_{\perp}, \nu_{////}, \nu_{//\perp}, G_{//\perp} \qquad\qquad b_{//}, b_{\perp}$$

- Plasticity :

Cohesion anisotropy with fabric tensor

$$c_0 = a_{ij}\, l_i\, l_j \qquad\qquad l_i = \sqrt{\frac{\sigma_{i1}^{'2} + \sigma_{i2}^{'2} + \sigma_{i3}^{'2}}{\sigma_{ij}^{'}\sigma_{ij}^{'}}}$$

Cross-anisotropy

$$c_0 = \bar{c}\left(1 + A_{////}(1 - 3l_2^2) + b_1 A_{////}^2 (1 - 3l_2^2)^2 + \dots\right)$$

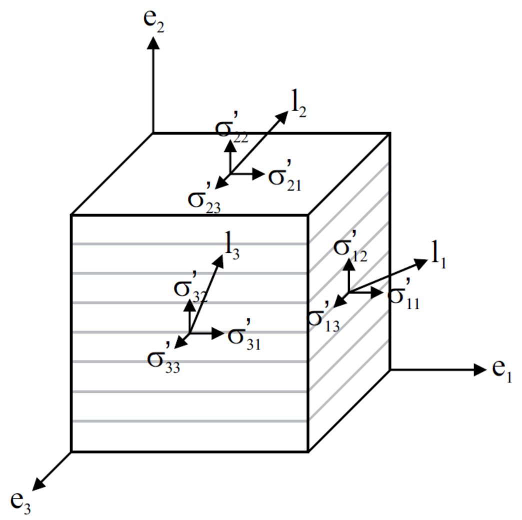

Excavation / Fracturation modelling

- Stress state

Major stress in the axial direction — $\sigma_{x,0} = \sigma_h = 12.40$ MPa

Gallery // to σ_H — $\sigma_{y,0} = \sigma_v = 12.70$ MPa

$\sigma_{z,0} = \sigma_H = 1.3 \times \sigma_h = 16.12$ MPa

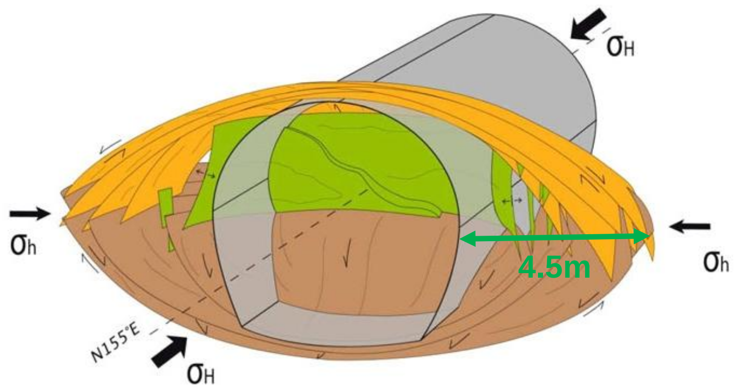

- Shear banding

Total deviatoric strain

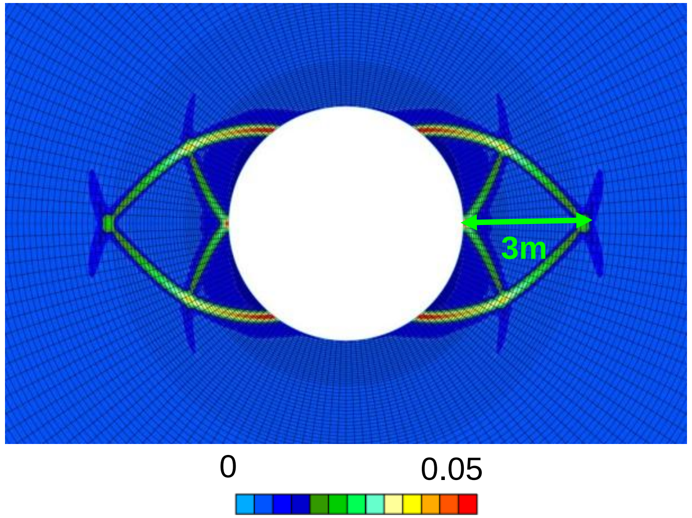

→ **Shape modification due to σ_H**

- Convergence

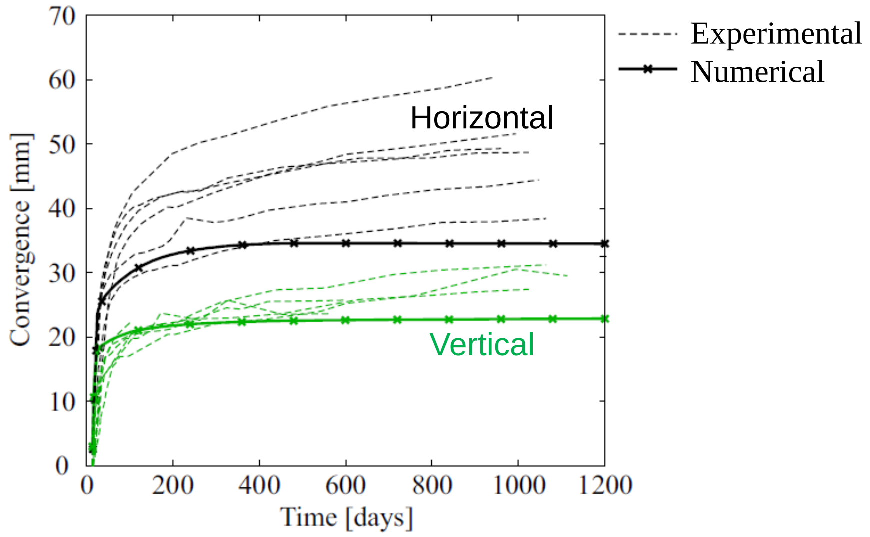

→ **Long-term deformation** → **Creep deformation**

Table of Contents

End of the story ?

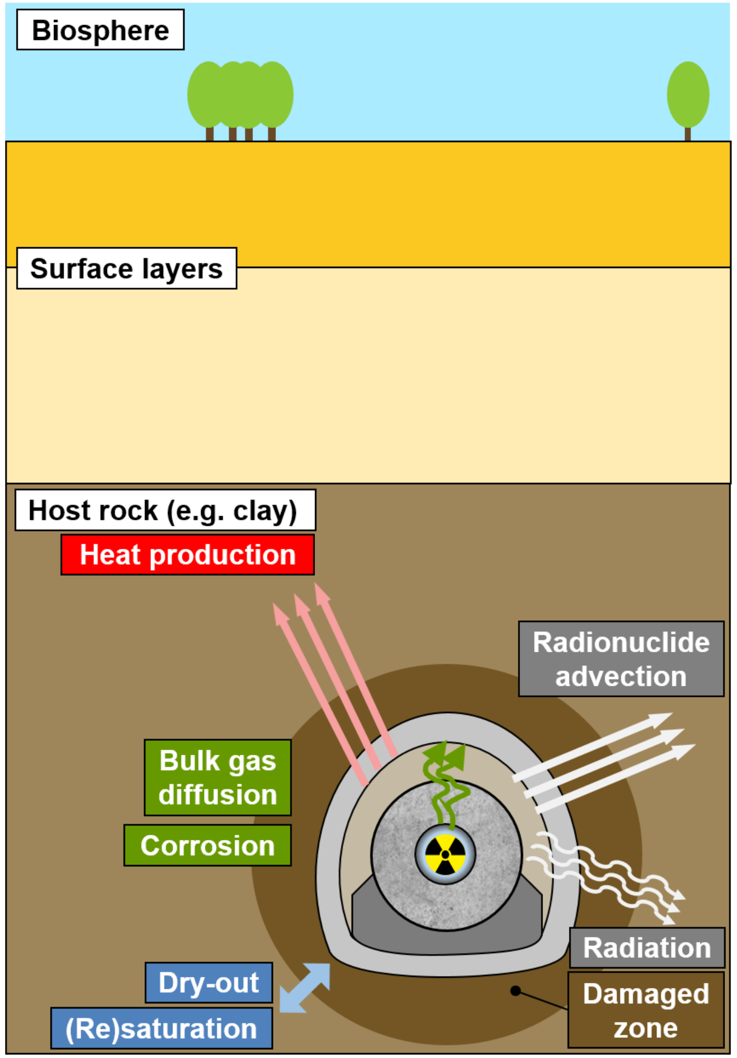

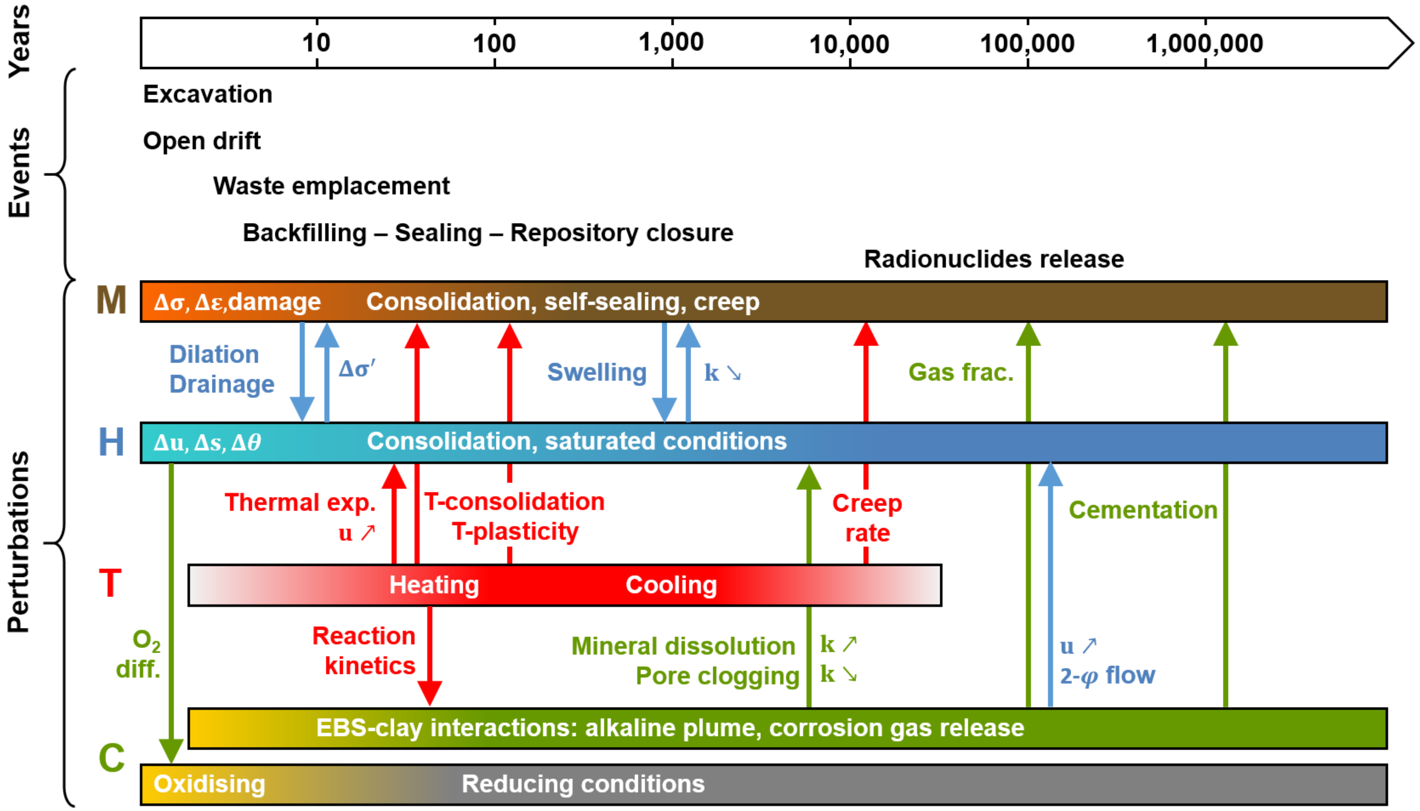

[Sillen, 2012].

LIÈGE université Urban & Environmental Engineering

Avec le soutien de la Wallonie

fnrs LA LIBERTÉ DE CHERCHER

Thank you for your attention.

This work is co-funded by the FNRS – Projet bilateral de Mobilité PINT-BILAT-M R.M008.23